Cellular/Molecular

Dendritic HCN2 Channels Constrain Glutamate-Driven Excitability in Reticular Thalamic Neurons

Shui-Wang Ying,[1] Fan Jia,[1] Syed Y. Abbas,[1] Franz Hofmann,[2] Andreas Ludwig,[3] and Peter A. Goldstein[1]

[1]C. V. Starr Laboratory for Molecular Neuropharmacology, Department of Anesthesiology, Weill Medical College, Cornell University, New York, New York 10021, [2]Institut für Pharmakologie und Toxikologie, 80802 München, Germany, and [3]Institut für Experimentelle und Klinische Pharmakologie und Toxikologie, Friedrich-Alexander-Universität Erlangen-Nürnberg, 91054 Erlangen, Germany

Hyperpolarization activated cyclic nucleotide (HCN) gated channels conduct a current, I_h; how I_h influences excitability and spike firing depends primarily on channel distribution in subcellular compartments. For example, dendritic expression of HCN1 normalizes somatic voltage responses and spike output in hippocampal and cortical neurons. We reported previously that HCN2 is predominantly expressed in dendritic spines in reticular thalamic nucleus (RTN) neurons, but the functional impact of such nonsomatic HCN2 expression remains unknown. We examined the role of HCN2 expression in regulating RTN excitability and GABAergic output from RTN to thalamocortical relay neurons using wild-type and HCN2 knock-out mice. Pharmacological blockade of I_h significantly increased spike firing in RTN neurons and large spontaneous IPSC frequency in relay neurons; conversely, pharmacological enhancement of HCN channel function decreased spontaneous IPSC frequency. HCN2 deletion abolished I_h in RTN neurons and significantly decreased sensitivity to 8-bromo-cAMP and lamotrigine. Recapitulating the effects of I_h block, HCN2 deletion increased both temporal summation of EPSPs in RTN neurons as well as GABAergic output to postsynaptic relay neurons. The enhanced excitability of RTN neurons after I_h block required activation of ionotropic glutamate receptors; consistent with this was the colocalization of HCN2 and glutamate receptor 4 subunit immunoreactivities in dendritic spines of RTN neurons. The results indicate that, in mouse RTN neurons, HCN2 is the primary functional isoform underlying I_h and expression of HCN2 constrains excitatory synaptic integration.

Key words: **I_h block; HCN2 knock-out; synaptic integration; RTN; immunohistochemistry; AMPA receptor**

Introduction

Hyperpolarization activated cyclic nucleotide (HCN) gated channels conduct a current, I_h, that contributes to multiple membrane properties governing cellular excitability (Pape, 1996; Gauss and Seifert, 2000; Robinson and Siegelbaum, 2003). HCN channels are unevenly distributed on the cell membrane; for example, HCN1 is preferentially expressed on distal dendritic membranes of pyramidal cells in the cortex, hippocampus, and subiculum (Lörincz et al., 2002). Consistently, dendritic I_h current density and amplitude increases as one moves farther away from the soma (Magee, 1998; Williams and Stuart, 2000; Berger et al., 2001; Kole et al., 2006). Dendritic I_h normalizes temporal summation (Stuart and Spruston, 1998; Magee, 1999; Berger et al., 2001; Koch and Grothe, 2003), disconnects somatic and dendritic spike initiation zones (Berger et al., 2003), and likely limits the development of long-term potentiation (Nolan et al., 2004).

HCN2 and HCN4 are the two major isoforms present in the thalamic reticular nucleus (RTN) (Notomi and Shigemoto, 2004), but the relative contribution of the two isoforms to I_h in RTN neurons is unknown. Somatic I_h in RTN neurons is small even at hyperpolarized membrane potentials (Abbas et al., 2006; Rateau and Ropert, 2006). We previously demonstrated that HCN2 is preferentially expressed in the dendritic spines of RTN neurons (Abbas et al., 2006). The small somatic I_h recorded in these neurons may reflect current generation at sites distant from the soma (as in dendritic spines) and subsequent signal attenuation resulting from a large dendritic electrotonic length (Destexhe et al., 1996).

Given that dendritic spines are important in regulating neuronal excitability and synaptic plasticity (Yuste and Tank, 1996; Hering and Sheng, 2001; Kasai et al., 2003; Tsay and Yuste, 2004; Carlisle and Kennedy, 2005; Segal, 2005), it is possible that I_h might be involved in the integration of excitatory synaptic input in the RTN. In RTN neurons, a significant proportion of the excitatory synaptic response is mediated by AMPA receptors containing the glutamate receptor 4 (GluR4) subunit (Mineff and Weinberg, 2000; Golshani et al., 2001). We hypothesized that HCN2 channels generated a distant I_h conductance that functioned as a leak current path to shunt excitatory inputs (Robinson and Siegelbaum, 2003). In this study, we investigated the contri-

Received Dec. 22, 2006; revised June 27, 2007; accepted June 27, 2007.

This work was supported by National Institutes of Health Grant GM066840 (P.A.G.). We thank Willie H. Mark (Developmental Biology Program, Sloan-Kettering Institute, Memorial Sloan-Kettering Cancer Center, New York, NY), Felix Wolf [Research Animal Resource Center (RARC), Weill Medical College, Cornell University, New York, NY], and the RARC staff for their assistance with the rederivation and maintenance of the mouse breeding colony. We also thank Alison North, Shivaprasad Bhuvanendran, and Mathieu Marchand, from the Rockefeller University Bio-Imaging Resource Center (New York, NY), for help with confocal microscopy and image analysis. Finally, we thank Neil Harrison for his thoughtful comments during the course of these experiments.

Correspondence should be addressed to Dr. Peter A. Goldstein, Department of Anesthesiology, Weill Medical College, Cornell University, 1300 York Avenue, Room A-1050, New York, NY 10021. E-mail: pag2014@med.cornell.edu.

DOI:10.1523/JNEUROSCI.1630-07.2007

 0270-6474/07/278719-14$15.00/0

bution of HCN2 channels to I_h generation in RTN neurons as well as their role in regulating excitability and synaptic integration in these cells using wild-type (+/+) and HCN2 deletion (−/−) mice. Because the overwhelming majority of excitatory synaptic transmission in the CNS occurs at dendritic spines (Nimchinsky et al., 2002), we also examined whether GluR4 colocalized with HCN2 in dendritic spines.

We found that HCN2 was the major isoform generating I_h in RTN because HCN2 deletion abolished I_h and recapitulated the effects of the I_h blocker ZD7288 (4-ethylphenylamino-1,2-dimethyl-6-methylaminopyrimidinium chloride). Functional expression of HCN2 in RTN constrained intrinsic excitability and ionotropic glutamate receptor-mediated synaptic integration, thereby reducing spike-dependent GABAergic output. Colocalization of HCN2 channels and the AMPA receptor GluR4 subunit was evident in the spines of RTN neurons, thus providing a structural basis for an interaction between intrinsic and synaptic conductances.

Materials and Methods

Genotyping. HCN2 knock-out mice were rederived from an established line (Ludwig et al., 2003) using standard techniques (Nagy et al., 2003). Mice were genotyped by Southern blot analysis as described previously (Ludwig et al., 2003) or by Transnetyx (Memphis, TN). Briefly, for mice genotyped by Transnetyx, tissue samples were lysed using Proteinase K, and DNA was isolated using the proprietary microbead-based method by Transnetyx. The DNA was then tested in duplicate using a specific quantitative PCR assay with results normalized to a single-copy housekeeping gene.

Electrophysiology. Experiments were performed in accordance with institutional and federal guidelines. Acute brain slice preparation and whole-cell voltage- and current-clamp recording techniques have been described previously in detail (Ying and Goldstein, 2005a,b). Briefly, mice [postnatal day 55 (P55) to P85] were anesthetized with halothane and decapitated, and horizontal or thalamocortical slices (220 or 300 μm) were cut on a microslicer (VT 1000S; Leica, Bannockburn, IL) using ice-cold slicing solution, which contained the following (in mM): 2 KCl, 26 $NaHCO_3$, 1.25 NaH_2PO_4, 240 sucrose, 12 glucose, 2 $MgSO_4$, 1 $MgCl_2$, and 1 $CaCl_2$. Whole-cell patch-clamp recordings from visually identified neurons in the ventrobasal (VB) complex and RTN were made from brain slices at 22–23°C using either a Multiclamp 700B or Axopatch 200A amplifier (Molecular Devices, Foster City, CA). Access resistance (R_a) was compensated by up to 80% and ranged from 5 to 8 MΩ after compensation; data were discarded if R_a increased by >20%. Typically, neurons that had a resting membrane potential (RMP) negative to −60 mV (when measured immediately after rupturing the gigaohm seal) and had an input resistance (R_{in}) >180 MΩ were selected for study; also included for analysis were a subgroup of RTN neurons that showed spontaneous tonic spike firing at membrane potentials between −52 and −48 mV. To study drug effects on tonic spike firing in RTN neurons, the membrane potential was initially adjusted to −51 to −50 mV using intracellular injection of direct current except when testing various potassium channel blockers, in which case the resting membrane potential was used. For simultaneous recordings of tonic spike firing in RTN and VB neurons, the initial membrane potential was set to approximately −44 mV for each group of cells. Steady-state R_{in} was measured at a holding membrane potential level close to RMP from the voltage response elicited by injection of a small hyperpolarizing current (−30 pA, 500 ms). Liquid junction potentials were calculated and corrected off-line.

Slices were perfused with carbogenated artificial CSF, which contained the following (in mM): 117 NaCl, 25 $NaHCO_3$, 3.6 KCl, 1.2 NaH_2PO_4, 1.2 $MgCl_2$, 2.5 $CaCl_2$, and 12 glucose; osmolarity was adjusted to 300 mOsm

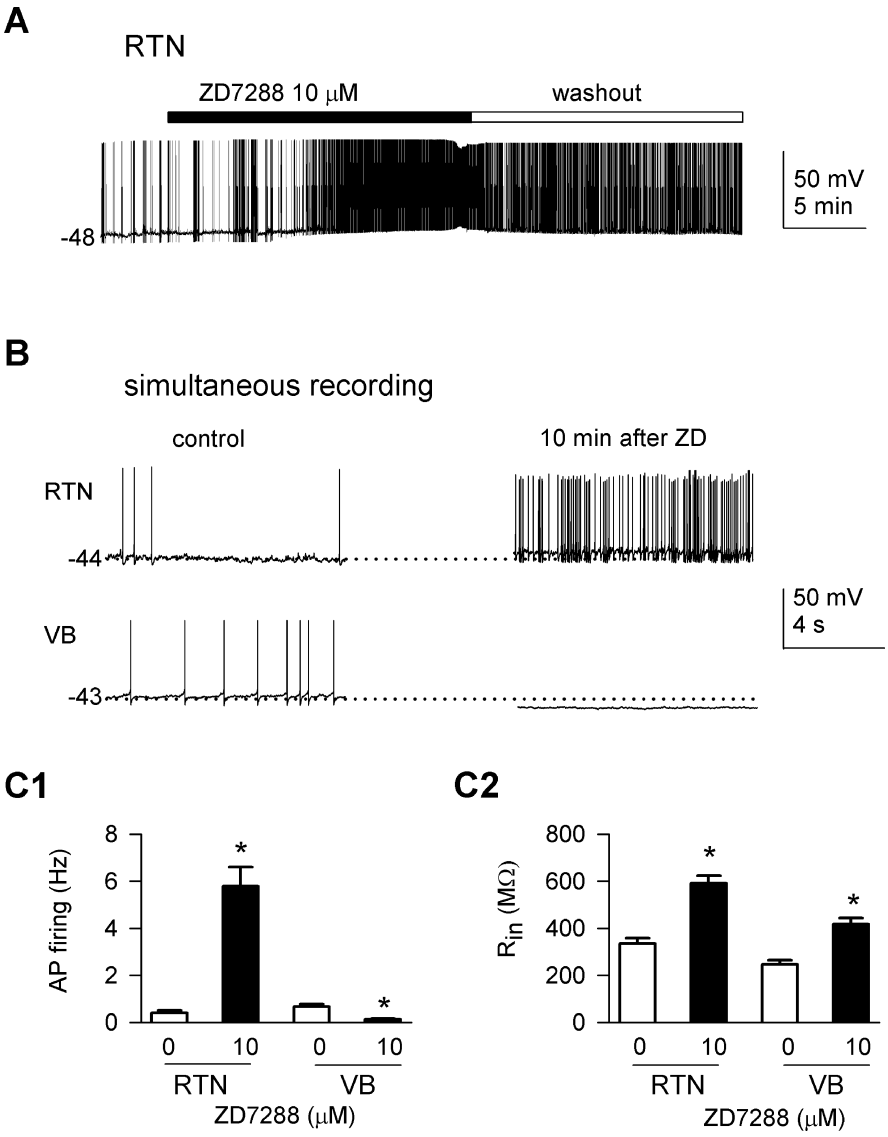

Figure 1. Blockade of HCN channels increases the spike firing rate in RTN, but not VB, neurons. ***A***, Application of the HCN channel blocker ZD7288 increases spontaneous action potential (AP) firing in an RTN neuron. The value to the left of the trace indicates membrane potential level (in millivolts) in this and subsequent figures. ***B***, Simultaneous recordings of an RTN and VB neuron demonstrate that ZD7288 affects action potential firing in a nucleus-specific manner. Representative traces show firing activity before (left) and 10 min (right) after ZD7288 (10 μM) application. ZD7288 increased action potential firing in the RTN neuron but decreased it in the VB neuron. The thin dotted line indicates the level of the membrane potential at the start of the first trace; note the small depolarization in the membrane potential in the RTN neuron compared with the small hyperpolarization observed in the VB neuron. Bicuculline (10 μM) was present in the extracellular solution during simultaneous recordings to prevent rebound burst firing. ***C1***, Bar graph summarizing effect of ZD7288 on firing rate (hertz). *$p < 0.05$ (paired t test), 10 μM ZD7288 versus control (0 μM); $n = 22$ for RTN, $n = 10$ for VB. Data pooled from experiments described in ***A*** and ***B***. ***C2***, Bar graph summarizing effects of ZD7288 on R_{in}; same pooled data as ***C1***.

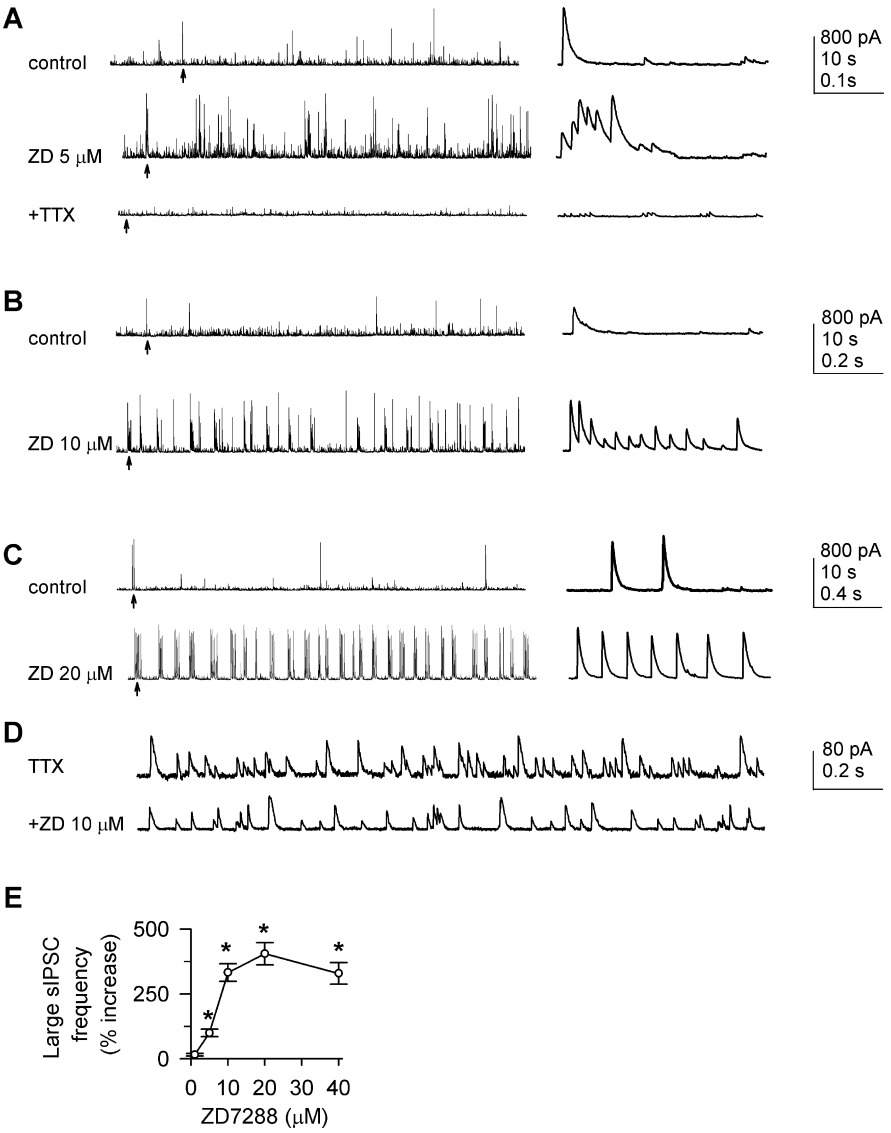

Figure 2. Blockade of HCN channels increases frequency of large-amplitude IPSCs in VB neurons. ***A***, Control sIPSCs were recorded from a VB neuron; ZD7288 (ZD) at 5 μM increases the sIPSC frequency, and addition of TTX (1 μM) abolishes all large sIPSCs, indicating that these large sIPSCs are action potential dependent. Representative events (marked by arrows) are expanded on the right in this and the following panels. Timescale: 10 s for traces on left; 0.1 s for expanded traces (right). ***B***, ***C***, ZD7288 at 10 μM (***B***) and 20 μM (***C***) further increases large sIPSC frequency in different neurons. Timescale: 10 s for traces on left; 0.2 s for ***B***; and 0.4 s for ***C***, respectively, for expanded traces (right). ***D***, In a different neuron than above, mIPSCs are recorded in the presence of TTX (1 μM) followed by TTX plus ZD7288 (10 μM). Note the different scales for amplitude and time: 80 pA, 0.2 s here versus 800 pA, 0.1 s in ***A***. ***E***, Grouped data demonstrate that ZD7288 increases the large sIPSC frequency in a concentration-dependent manner. Frequency (hertz) at indicated ZD7288 concentrations were as follows (corresponding control values provided at each concentration): 1 μM, 2.96 $\pm$ 0.18 (2.56 $\pm$ 0.19); 5 μM, 5.14 $\pm$ 0.52 (2.46 $\pm$ 0.27); 10 μM, 9.67 $\pm$ 1.24 (2.23 $\pm$ 0.25); 20 μM, 12.97 $\pm$ 1.69 (2.56 $\pm$ 0.24); 40 μM, 9.71 $\pm$ 1.4 (2.25 $\pm$ 0.29). *$p < 0.05$ versus control.

with sucrose. For recordings of I_h currents, an "I_h isolation solution" was used, which contained the following (in mM): 114 NaCl, 26 $NaHCO_3$, 15 KCl, 1.25 $MgCl_2$, 2 $CaCl_2$, 11 D-glucose, 0.001 tetrodotoxin (TTX), 1 $BaCl_2$, 0.1 $NiCl_2$, 0.04 D-(−)-2-amino-5-phosphonopentanoic acid (D-AP-5), and 0.02 6-cyano-7-nitroquinoxaline-2,3-dione (CNQX) (Abbas et al., 2006; Rateau and Ropert, 2006). For recordings of I_h currents and voltage responses, the pipette solution contained the following (in mM): 135 K^+-gluconate, 5 NaCl, 10 HEPES, 0.5 EGTA, 2 ATP-Mg^{2+}, 0.3 GTP-Na^+, and 10 Na_2-phosphocreatine, the pH adjusted to 7.3 with KOH. For recordings of IPSCs, the pipette solution contained the following (in mM): 130 CH_3SO_3Cs, 8.3 CH_3SO_3Na, 1.7 NaCl, 1 $CaCl_2$, 10 EGTA, 2 Mg_2-ATP, 0.3 Na-GTP, and 10 HEPES, pH adjusted to 7.2 with CsOH. Bath and focal application of drugs was performed as described previously (Ying and Goldstein, 2005a). ZD7288 was applied by bath superfusion for at least 10 min before data collection unless otherwise noted. In a number of experiments, to test for a direct effect on RTN neurons, a solution containing ZD7288 (20–40 μM) was focally ejected (2–5 psi) onto an RTN neuron through a puffer pipette connected to a Picospritzer II (Parker Instruments, Fairfield, NJ).

Data were collected at least 10 min after obtaining whole-cell access to allow the pipette solution to equilibrate with the neuron. For recording I_h currents, neurons were voltage clamped at −40 mV, and voltage steps (10 s, 10 mV/step) were applied from −40 to −120 mV. In a number of instances, a single 20 s step to −110 mV was also applied. Spontaneous IPSCs (sIPSCs) and miniature IPSCs (mIPSCs) were recorded as described previously (Ying and Goldstein, 2005a).

Extracellular electrical stimulation. Corticothalamic stimulation to evoke EPSPs in RTN neurons or RTN stimulation to evoke IPSCs in VB neurons has been described previously (Ying and Goldstein, 2005a,b). Briefly, to evoke EPSPs in RTN neurons, a concentric bipolar tungsten electrode (Frederick Haer Company, Bowdoinham, ME) was placed in the internal capsule in thalamocortical slices. Our previous experiments indicated that, in addition to membrane and input resistance, evoked EPSP parameters (amplitude and time constant) are dependent on stimulus current intensity and duration, as well as the distance between recording and stimulation sites. To minimize interneuronal variability and to facilitate comparisons between data obtained from wild-type and HCN2 knock-out animals (Nolan et al., 2004), care was taken to keep stimulation parameters (and distance) constant. The stimulating electrode was positioned using a fine adjustment microdrive (after whole-cell configuration was obtained) so that evoked EPSPs occurred with a latency of 2.7–2.8 ms (2.76 $\pm$ 0.03 ms; $n = 30$ neurons), while stimulation intensity (298 μA) and duration (0.1 ms) were kept constant. Under control conditions, the variability in EPSP amplitude and decay time within same group (wild-type or HCN2 knock-out) of neurons was not significant. To evoke IPSCs in VB neurons, the stimulation electrode was placed in RTN (at somatosensory sector) or the internal capsule. Each cell served as its own control.

Single pulses were delivered using a Master-8 pulse generator (A.M.P.I., Jerusalem, Israel), and stimulus intensity was controlled by a constant-current stimulus isolator (World Precision Instruments, Sarasota, FL). Responses were considered monosynaptic if the latency jitter was <0.4 ms and their rise times were consistent from trial to trial (three trials). To confirm that responses were $GABA_A$ receptor mediated, a $GABA_A$ receptor antagonist (bicuculline at 10 μM or gabazine at 10 μM) was used to block responses in the presence of a $GABA_B$ receptor antagonist (2-OH-saclofen at 100 μM). CNQX (20 μM) and D-AP-5 (40 μM) were used to identify AMPA and NMDA receptor-mediated components of the EPSP, respectively.

Data analysis. Analysis of I_h currents and membrane voltage responses were performed using MiniAnalysis (Synaptosoft, Decatur, GA) or Clampfit as described previously (Ying and Goldstein, 2005a,b; Abbas et

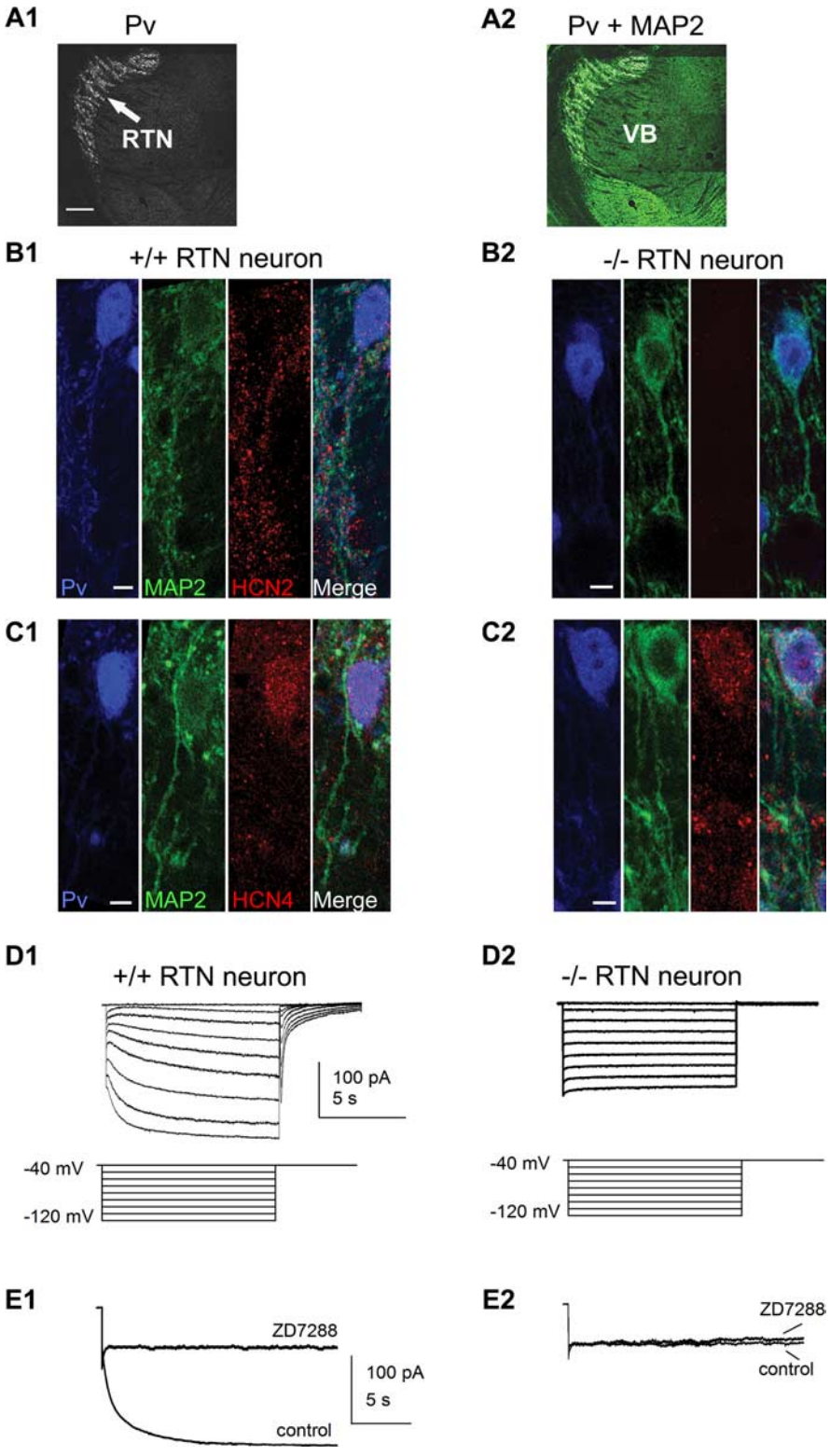

Figure 3. HCN2 is the major isoform that generates I_h in RTN neurons. ***A1***, Low-magnification confocal microscopy image shows immunofluorescence for parvalbumin (Pv; white) labeling RTN neurons in the thalamus. Scale bars: ***A1***, 200 μm; ***B1***, ***C1***, 5 μm. ***A2***, MAP2 expression (green) is present in parvalbumin-positive GABAergic neurons, as assessed by double immunofluorescence. ***B1***, High-magnification images show triple-immunofluorescent labeling for parvalbumin (blue), MAP2 (green), and HCN2 (red) in a +/+ RTN neuron. Note that very little HCN2-IR is present on the RTN cell body densely labeled with parvalbumin. In the merged image, there is no apparent colocalization between HCN2-IR and MAP2-IR. ***B2***, HCN2 immunolabeling is absent in −/− RTN neurons. ***C1***, Immunostaining with antibodies against HCN4 shows prominent somatic labeling in the +/+ RTN neuron. ***C2***, A similar HCN4 expression pattern is seen in a −/− RTN neuron. Merged images demonstrate that labeling for HCN4 and MAP2 does not overlap in +/+ (***C1***) and −/− (***C2***) RTN neurons. ***D1***, ***D2***, Whole-cell voltage-clamp recordings show a family of current traces recorded from a +/+ RTN neuron (***D1***); the voltage protocol is shown below. HCN2 deletion (***D2***) eliminates I_h currents in the RTN neuron. ***E1***, ***E2***, Exemplar current traces in response to a 20-s-long voltage step to −110 mV (from −40 mV; protocol not shown) in +/+ (***E1***) and −/− (***E2***) RTN neurons. A ZD7288-sensitive current is readily detected in the +/+, but not −/−, RTN neuron.

al., 2006; Ying et al., 2006a). Data are presented as mean ± SEM; statistical significance was determined using Student's *t* test or one-way ANOVA with pairwise comparisons when appropriate.

Immunohistochemistry. Immunohistochemistry techniques for HCN channel labeling were modified from those described previously (Abbas et al., 2006). Briefly, wild-type (+/+) and HCN2 knock-out (−/−) mice of the same age (P28–P35) were used. Brain slices containing the RTN (and other structures) were sectioned at 20 μm at a 45° angle using a vibrating microtome (Leica). After extensive rinsing in PBS (100 mM, pH 7.4) and permeabilization with 0.1% Triton X-100 in PBS for 15 min, free-floating brain slices from +/+ and −/− mice were processed simultaneously for triple immunofluorescence labeling (Abbas et al., 2006). A blocking solution (10% donkey serum prepared in PBS) was used to minimize nonspecific binding before incubation of slices in a primary antibody. Brain slices were incubated in the dark with primary antibodies at 4°C overnight.

GABAergic neurons in RTN were labeled using anti-parvalbumin mouse antibody (1:1000 dilution; PARV-19, Sigma, St. Louis, MO). Anti-HCN2 and anti-HCN4 rabbit antibodies (1:40 dilution; Alomone Labs, Jerusalem, Israel) were used to detect immunoreactivity (IR) for the corresponding HCN isoforms. Dendrites were identified using a monoclonal anti-microtubule-associated protein 2 (MAP2) mouse antibody (1:300 dilution; MAB364; Chemicon, Temecula, CA), and dendritic spines were identified using anti-cortactin rabbit antibody (1:200 dilution; sc-11408; Santa Cruz Biotechnology, Santa Cruz, CA). A polyclonal anti-GluR4 goat antiserum (1:50 dilution; sc-7614; Santa Cruz Biotechnology) was used to identify GluR4 subunits; the specificity of the anti-GluR4 antibody has been characterized previously (Mokin and Keifer, 2006). Secondary antibodies (from Jackson ImmunoResearch, West Grove, PA) used were: donkey anti-mouse cyanine 5 (Cy5) monovalent fab fragments (1:300 dilution), donkey anti-mouse Rhodamine Red-X IgG (heavy and light chain) (1:100 dilution), donkey anti-rabbit Cy5 IgG (heavy and light chain) (1:400 dilution), goat anti-rabbit FITC monovalent fab fragments (1:100 dilution), donkey anti-goat Alexa 488 IgG (heavy and light chain) (1:400 dilution; Invitrogen, Carlsbad, CA), and donkey anti-goat rhodamine monovalent fab fragments (1:100 dilution; Rockland, Gilbertsville, PA). All appropriate dilutions were performed in a blocking solution.

Confocal microscopy. Multichannel imaging was performed with a laser-scanning confocal microscope system (LSM510 mounted on an

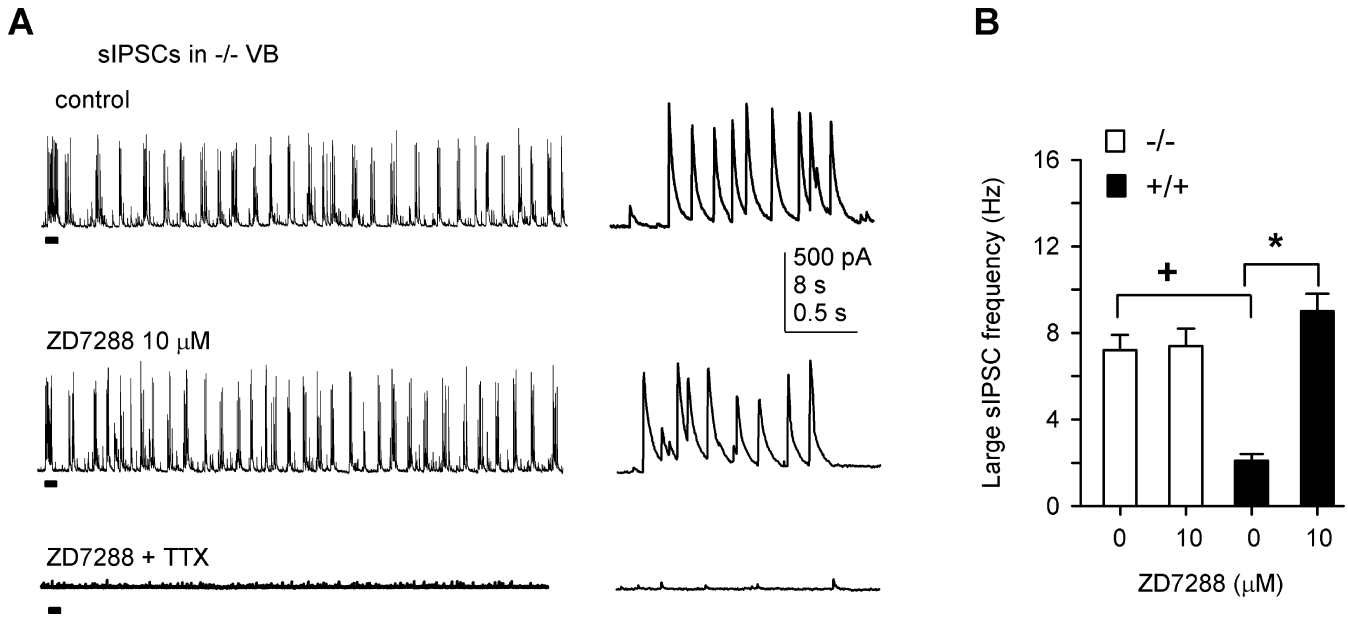

Figure 4. HCN2 deletion increases GABAergic output from RTN to VB and abolishes sensitivity to ZD7288. ***A***, sIPSCs are recorded from a −/− VB neuron. ZD7288 (10 μM) fails to affect sIPSC frequency, and addition of TTX (1 μM) eliminates all large sIPSCs in the same neuron. sIPSCs marked by solid bars are expanded on right. Calibration: 500 pA for all traces; 8 s and 0.5 s for traces on left and right, respectively. ***B***, Bar graph summarizing effects of ZD7288 and comparison of large sIPSC frequency between +/+ and −/− VB neurons. *$p < 0.05$, 10 μM ZD7288 versus control (0 μM) in +/+ VB neurons ($n = 20$). $^{+}p < 0.05$, control in +/+ versus control in −/− VB neurons ($n = 20$).

Axiovert 200; Zeiss, Oberkochen, Germany) fit with 63×/1.2 numerical aperture water-immersion and 20× objectives, as described previously (Abbas et al., 2006). The pinhole diameter was set to 1 airy unit (1.2 μm). Twelve bit images were captured using LSM 510 Image Browser version 3.2, and *Z* sections were obtained at 1.0 μm intervals. Laser and detector settings were retained for all images collected within experimental groups. Captured images from optical sections were arranged and processed using Imaris version 4.2 (Bitplane, St. Paul, MN). Figures were constructed using Adobe Photoshop (Adobe Systems, San Jose, CA).

Chemicals. Salts were from Sigma (St. Louis, MO) unless otherwise noted. ZD7288, (+)-bicuculline, 2-OH-saclofen, CNQX, and D-AP-5 were obtained from Tocris Bioscience (Ellisville, MO), and TTX was from Alomone Labs.

Results

I_h regulates excitability and spike firing in RTN neurons

We demonstrated previously that the HCN2 channel isoform is present in dendritic spines at a very high density, whereas somatic I_h amplitude and voltage sag are small in RTN neurons (Ying and Goldstein, 2005a; Abbas et al., 2006). The distal localization of HCN2 in RTN might influence somatic excitability and spike firing, and this possibility was first examined by blocking HCN channels. Action potential firing was recorded under control conditions in RTN neurons ($n = 10$) that fired spontaneously; bath application of ZD7288 produced a modest depolarization in the membrane potential and dramatically increased spike firing (Fig. 1*A*). The increased firing activity did not completely recover to the control (predrug) level even after 30 min washout. In another group of RTN neurons ($n = 6$) that did not fire spontaneously, spike firing was initiated by intracellular injection of direct current (DC) (50–80 pA) throughout recordings in the absence and presence of ZD7288. Effects of ZD7288 were similar on spontaneous and DC-initiated firing patterns and are included in Figure 1, *C1* and *C2*. In addition, focal application of ZD7288 (20 μM in puffer pipette) also markedly increased spike firing ($n = 3$; traces not shown).

Effects of ZD7288 are nucleus specific

RTN and VB neurons have distinct compartmental expression patterns for HCN2 (Abbas et al., 2006), and those differences might lead to a nucleus-specific response to ZD7288. Accordingly, we examined whether the ZD7288-induced depolarization observed above was nucleus specific, reflecting differences in the subcellular distribution of HCN2 and HCN4 channels (Abbas et al., 2006), rather than an artifact attributable to drift in the membrane potential. To test this, we performed simultaneous recordings in RTN and VB neurons. Spike firing in both RTN and VB neurons was initiated with intracellular injection of DC to nearly identical initial membrane potentials in the presence of bicuculline. Representative traces from simultaneous recordings are shown in Figure 1*B*.

Data from RTN neurons in single and simultaneous recordings were similar and pooled for statistical analyses; pooled data indicate that ZD7288 (10 μM) significantly increased the spike firing rate in RTN neurons (0.3 ± 0.1 Hz in control vs 6.3 ± 0.8 Hz in ZD7288; $n = 22$; $p < 0.001$) (Fig. 1*C1*) as well as R_{in} (336 ± 22 vs 592 ± 32 MΩ; $p < 0.05$; note that these values were obtained in the absence of AP-5 and CNQX) (Fig. 1*C2*) and significantly depolarized the membrane by 5.8 ± 2.1 mV. In contrast, ZD7288 hyperpolarized the membrane potential by 8.2 ± 3.1 mV ($n = 10$) and significantly decreased firing (0.67 ± 0.12 Hz in control and 0.13 ± 0.03 Hz in ZD7288) in VB neurons (Fig. 1*C1*,*C2*); however, R_{in} still increased in the presence of ZD7288 (246 ± 18 and 418 ± 26 MΩ in control and ZD7288, respectively; $p < 0.05$). The percentage increase in R_{in} after ZD7288 application was similar in both neuronal types (increase from pooled data, 76.2 ± 8% for RTN and 70 ± 10% for VB neurons).

Blockade of HCN channels increases the frequency of large sIPSCs in VB neurons

The increased excitability attributable to HCN channel blockade in GABAergic RTN neurons should presumably increase the fre-

quency of sIPSCs in VB neurons because the RTN is the sole source of GABA release in the rodent VB (Arcelli et al., 1997); thus, we examined effects of ZD7288 on the frequency of large-amplitude (>100 pA) sIPSCs in VB neurons. ZD7288 (1 μM) nominally increased sIPSC frequency (traces not shown) and, at 5 μM, markedly increased the occurrence of large sIPSCs (Fig. 2*A*). Addition of TTX abolished all large sIPSCs, indicating that the large sIPSCs induced by ZD7288 were spike dependent. At higher concentrations (10 and 20 μM), ZD7288 induced large, "bursting" sIPSCs in different neurons (Fig. 2*B*,*C*). Grouped data indicate that ZD7288 increased the large sIPSC frequency in a concentration-dependent manner (Fig. 2*E*); the percentage increases were 16.3 ± 5% (1 μM; $n = 5$), 109 ± 12% (5 μM; $n = 10$), 334 ± 33% (10 μM; $n = 15$), 405 ± 36% (20 μM; $n = 15$), and 330 ± 36% (40 μM; $n = 10$). In addition, application of a different HCN blocker, Cs^+ (1 mM, 10 min), also significantly increased large sIPSC frequency (percentage increase, 190 ± 20%; $n = 6$; traces not shown).

To examine whether ZD7288 affected spike-independent release of GABA, mIPSCs were recorded from VB neurons in the presence of 1 μM TTX. Neither the frequency nor amplitude of mIPSCs was affected by 10 μM ZD7288 (Fig. 2*D*). mIPSC amplitude was 63.1 ± 3.8 and 58.1 ± 3.4 pA in control and ZD7288, respectively; mIPSC frequency was 22.1 ± 2.6 and 19.4 ± 2.9 Hz in control and ZD7288, respectively (data from eight cells). All IPSCs could be completely blocked by the $GABA_A$ receptor antagonist gabazine (traces not shown).

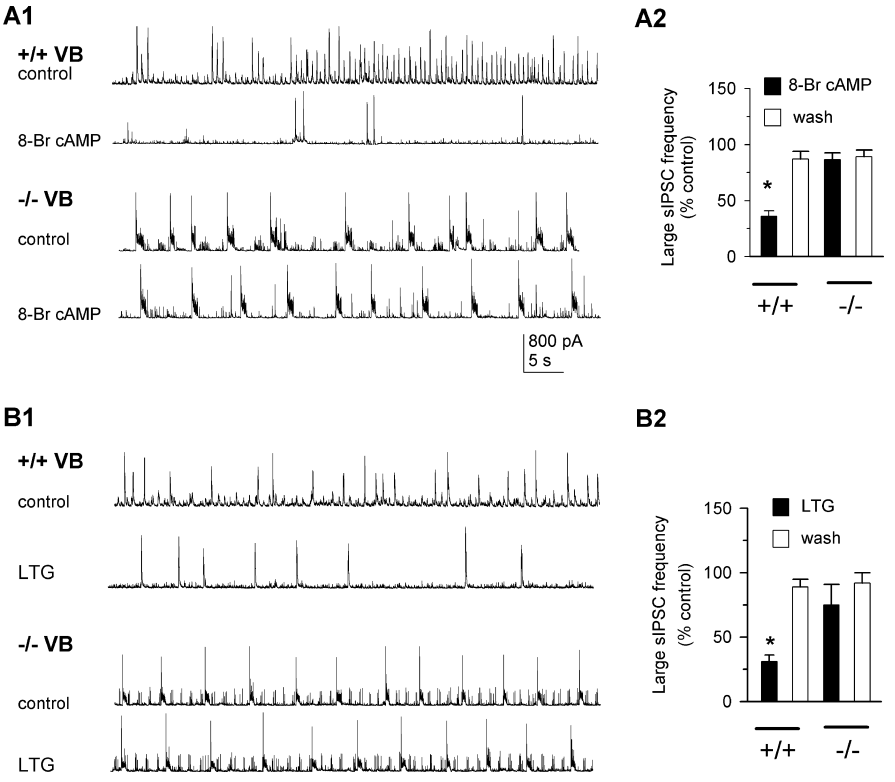

Figure 5. HCN2 in RTN restrains GABAergic output. ***A1***, In an HCN2 +/+ VB neuron, enhancing HCN channel function by 8-Br-cAMP (200 μM) superfusion decreases large sIPSC frequency, but this effect is absent in a −/− VB neuron. Recordings for control (predrug) and 8-Br-cAMP are made from the same neuron. Traces for washout are not shown. ***A2***, Bar graph indicates shows that 8-Br-cAMP reversibly reduces large sIPSC frequency in +/+, but not −/−, VB neurons. For +/+ neurons, sIPSC frequency (hertz) was as follows: control, 2.84 ± 0.24; 8-Br-cAMP, 1.02 ± 0.09; and washout, 2.56 ± 0.22. For −/− neurons, sIPSC frequency was as follows: control, 7.27 ± 0.47; 8-Br-cAMP, 6.39 ± 0.41; and washout, 6.55 ± 0.42. *$p < 0.05$ versus control, $n = 8$ each. ***B1***, ***B2***, Another HCN channel modulator lamotrigine (LTG; 50 μM) also decreases large sIPSC frequency in +/+, but not HCN −/−, VB neurons (***B1***). ***B2***, For +/+ neurons, sIPSC frequency (hertz) was as follows: control, 2.54 ± 0.27; lamotrigine, 0.79 ± 0.08; and washout, 2.35 ± 0.32. For −/− neurons, sIPSC frequency was as follows: control, 8.38 ± 1.14; lamotrigine, 7.36 ± 1.0; and washout, 7.55 ± 1.03. *$p < 0.05$ versus control, $n = 8$. Traces for control and LTG are from the same neuron.

In another subgroup of VB neurons (traces not shown), IPSCs were evoked by extracellular stimulation of the RTN. ZD7288 (10 or 20 μM) did not significantly change the evoked current amplitude (percentage control, 91 ± 6 and 84 ± 7%, respectively; $n = 5$). Thus, changes in sIPSC frequency after ZD7288 application are unlikely to have resulted from modification of postsynaptic $GABA_A$ receptors in VB neurons.

HCN2 is the major isoform that generates I_h currents in mouse RTN neurons

Previous studies have shown that HCN2 and HCN4 are the major isoforms expressed in RTN (Notomi and Shigemoto, 2004), and HCN2 deletion does not lead to compensatory changes in the other HCN isoforms (Ludwig et al., 2003). Using both wild-type (+/+) and HCN2 knock-out (−/−) mice, we investigated the relative contribution of the two major HCN isoforms to I_h generation in RTN neurons.

Confocal microscopy images (Fig. 3*B*) demonstrated punctate HCN2-IR in +/+ RTN neurons, with sparse somatic labeling (Fig. 3*B1*). In −/− RTN neurons, however, HCN2-IR was absent in all cellular compartments (Fig. 3*B2*). In contrast to the distribution of HCN2-IR, HCN4-IR clustered predominantly over the soma (Fig. 3*C1*). HCN2 deletion did not alter HCN4-IR (Fig. 3*C2*), consistent with previous findings (Ludwig et al., 2003).

Whole-cell voltage-clamp recordings readily detected the presence of I_h currents in +/+ RTN neurons using 10 s voltage steps (Fig. 3*D1*). Somatic I_h amplitude was 142 ± 22 pA ($n = 5$) at a voltage step from −40 to −120 mV, consistent with our previous observations (Abbas et al., 2006). In −/− RTN neurons, however, no I_h could be detected under the same conditions ($n = 10$) (Fig. 3*D2*). Conceivably, HCN4 channels could also contribute to I_h in RTN neurons (Santoro et al., 2000; Notomi and Shigemoto, 2004). Because activation of I_h mediated by HCN4 is very slow (Ludwig et al., 1999; Seifert et al., 1999; Ishii et al., 2001; Stieber et al., 2003), we also used a long-duration (20 s) voltage step protocol to allow for adequate activation of the current. At −110 mV, the I_h amplitude was 152 ± 12 pA ($n = 5$) in +/+ RTN neurons (example trace shown in Fig. 3*E1*). Again, no apparent I_h could be detected in HCN2 −/− RTN neurons ($n = 5$) (example trace shown in Fig. 3*E2*). It is highly unlikely, therefore, that HCN4 contributes to I_h currents in RTN neurons.

HCN2 deletion abolishes effects of ZD7288 on GABAergic output from RTN

The impact of HCN2 channel expression on GABAergic output was further examined using both +/+ and −/− mice. Experiments were performed as described for Figure 2, and only traces

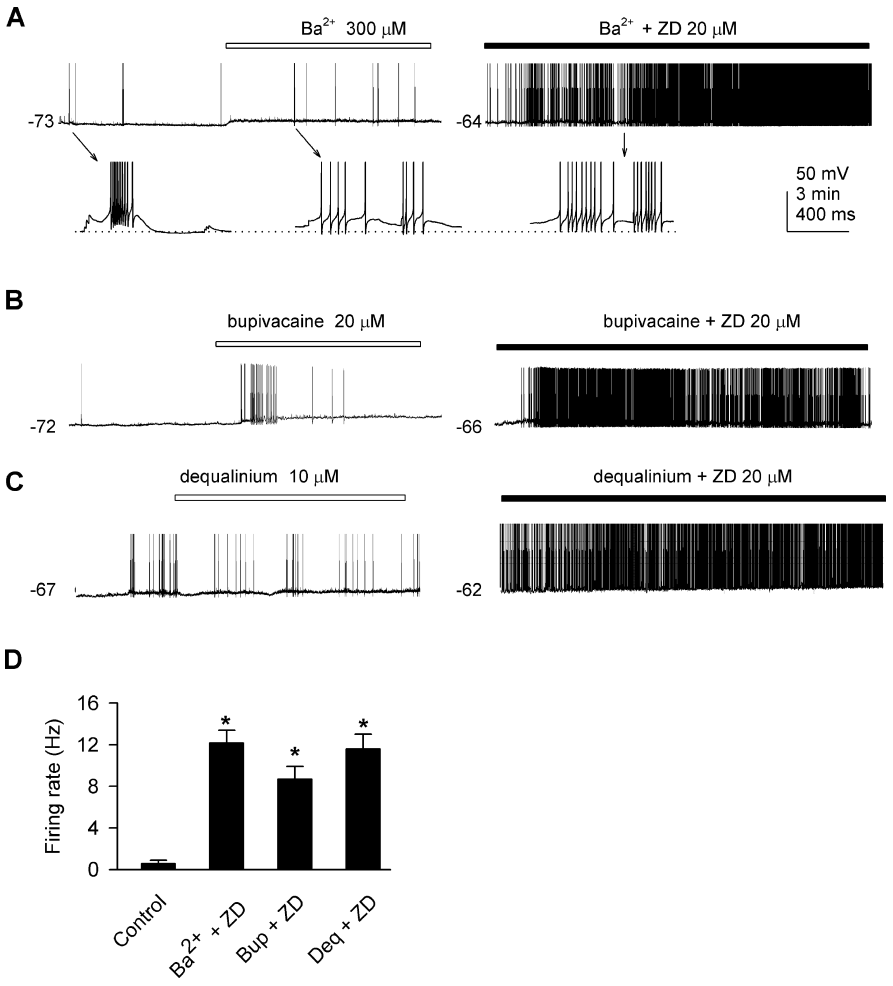

Figure 6. Potassium channel blockers do not occlude the effects of ZD7288 in RTN neurons. ***A***, Bath application of Ba^{2+} depolarizes the membrane potential, and addition of ZD7288 dramatically increases firing in the same +/+ neuron. Representative firing activities marked by arrows are expanded at bottom. The thin dotted line indicates the level of the membrane potential at the start of the first trace. Timescale: 3 min for top traces; 400 ms for expanded traces. ***B***, Application of the TASK channel blocker bupivacaine followed by addition of ZD7288 markedly increases firing. ***C***, Application of the SK channel blocker dequalinium does not occlude the response to ZD7288. ***D***, Bar graph summarizing effects of ZD7288 (ZD) on firing rate in the presence of Ba^{2+}, bupivacaine (Bup), and dequalinium (Deq), respectively. *$p < 0.05$ versus control, one-way ANOVA; $n = 10$ each.

for −/− mice are shown in Figure 4 (but data for +/+ mice are included in the group data). In contrast to +/+ mice, ZD7288 had no effect on large sIPSC frequency in −/− VB neurons; addition of 1 μM TTX confirmed that large sIPSCs were spike dependent (Fig. 4*A*). Grouped data (Fig. 4*B*) indicate that ZD7288 had little effect on large sIPSC frequency in HCN2 −/− VB neurons (7.2 ± 0.7 vs 7.4 ± 0.8 Hz for control and ZD7288, respectively), but in +/+ VB neurons the same concentration significantly increased the large sIPSC frequency (2.1 ± 0.3 Hz in control vs 9.1 ± 0.8 Hz in ZD7288; $p < 0.05$, one-way ANOVA with Tukey's test). In addition, deletion of HCN2 per se significantly increased large sIPSC frequency compared with control frequency in +/+ neurons (7.2 ± 0.7 Hz in −/− VB neurons vs 2.1 ± 0.3 Hz in +/+ VB neurons; $p < 0.05$) (Fig. 4*B*).

Enhancement of HCN channel function decreases GABAergic output from RTN to VB

cAMP strongly enhances HCN2 channel function (Ludwig et al., 1998; Chen et al., 2001b; Ulens and Tytgat, 2001; Wainger et al., 2001; Stieber et al., 2003), and I_h in RTN neurons is also sensitive to modulation by cAMP (Rateau and Ropert, 2006). We hypothesized that upregulation of HCN2 channel function might affect RTN excitability and, in turn, alter GABAergic output from RTN to VB. To test this hypothesis, sIPSC frequency was compared between +/+ and HCN2 −/− mice after superfusion of the membrane-permeable, nonhydrolysable cAMP analog, 8-bromo-cAMP (8-Br-cAMP).

Superfusion of 8-Br-cAMP (5 min) markedly decreased the frequency of large sIPSCs in +/+ VB neurons, although it had no effect in −/− VB neurons (Fig. 5*A1*); the inhibition of 8-Br-cAMP was reversible (traces not shown). Grouped data demonstrate that 8-Br-cAMP significantly decreased large sIPSC frequency in +/+ (percentage control, 36 ± 5%, $p < 0.05$ vs control, one-way ANOVA with Tukey's test) (Fig. 5*A2*) but not in −/− VB neurons (percentage control, 87.8 ± 6%).

The anticonvulsant lamotrigine also has been shown to enhance the I_h conductance, thereby decreasing the response of pyramidal neurons to synaptic inputs (Poolos et al., 2002; Berger and Lüscher, 2004). Using the same protocol as for 8-Br-cAMP, we examined the effect of lamotrigine on large IPSC frequency. Superfusion of lamotrigine (5 min) markedly reduced large sIPSC frequency in +/+, but not −/−, VB neurons (Fig. 5*B1*); the inhibition was also reversible (traces not shown). Grouped data demonstrate that lamotrigine application significantly reduced large sIPSC frequency in +/+ VB neurons (percentage control, 31.2 ± 5%) (Fig. 5*B2*) but had little effect on −/− VB neurons (percentage control, 92 ± 9%). The above data suggest that the HCN2 channel isoform expressed in RTN neurons is a key regulator of GABAergic output.

When glutamatergic transmission was blocked by AP-5 (40 μM) and CNQX (20 μM), the apparent periodicity of sIPSCs in HCN2 −/− VB neurons observed in Figure 5, *A* and *B*, is absent, and 8-Br-cAMP application still produced no significant change in sIPSC frequency (data not shown). The loss of bursting sIPSCs after block of excitatory synaptic transmission suggests that such activity may originate in a polysynaptic circuit, and this phenomenon requires additional study.

Excitatory effects of ZD7288 are not occluded by potassium channel blockers

The above data showed that ZD7288 depolarized the membrane potential in +/+ RTN neurons; this effect might be linked to modification of other conductances, especially potassium conductances, and thus this possibility was examined in +/+ RTN neurons. Spontaneous firing activity was recorded (a representative voltage trace is shown in Fig. 6*A*), and bath application of Ba^{2+}, a blocker of inwardly rectifying potassium conductances, depolarized the membrane potential by 8.6 ± 7 mV ($n = 10$) and

increased spike firing by 118 ± 22%; addition of ZD7288 further increased firing by 2600 ± 240% (compared with Ba^{2+}) (Fig. 6*D*).

At a low concentration (20 μM), the local anesthetic bupivacaine blocks TASK (TWIK-related acid-sensitive K^+ channels) channels in thalamic neurons (Meuth et al., 2003). Spontaneous spike firing was recorded in another group of RTN neurons, and bath application of bupivacaine (representative traces are shown in Fig. 6*B*) depolarized the membrane potential by 6.4 ± 3 mV ($n = 10$) and increased spike firing by 76 ± 9%. Addition of ZD7288 further increased firing by 2200 ± 198%.

The small-conductance Ca^{2+}-activated K^+ (SK) channel blocker dequalinium (Strøbaek et al., 2000) was similarly tested; bath application of dequalinium (10 μM, 10 min) (representative traces are shown in Fig. 6*C*) depolarized the membrane potential by 4.1 ± 2.2 mV ($n = 10$) and increased firing by 68 ± 15%. Coapplication of dequalinium and ZD7288 further increased the firing rate by 2400 ± 220%. None of the potassium channel blockers tested here were able to occlude the excitatory effects of ZD7288 on the spike firing rate in +/+ RTN neurons; therefore, it is unlikely that ZD7288 increased RTN spike firing as a result of an effect on these channels.

HCN2 channels attenuate synaptic integration in RTN neurons

RTN neurons receive massive excitatory glutamatergic input via descending corticothalamic fibers, and the excitatory response in these neurons is associated with densely expressed postsynaptic AMPA receptors, especially those containing the GluR4 subunit (Golshani et al., 2001). As shown in Figure 1, ZD7288 depolarized, rather than hyperpolarized, RTN neurons, and this might reflect the enhancement of excitatory synaptic integration in a manner similar to that mediated by HCN1 in the hippocampus (Nolan et al., 2004, their Fig. 7*B*).

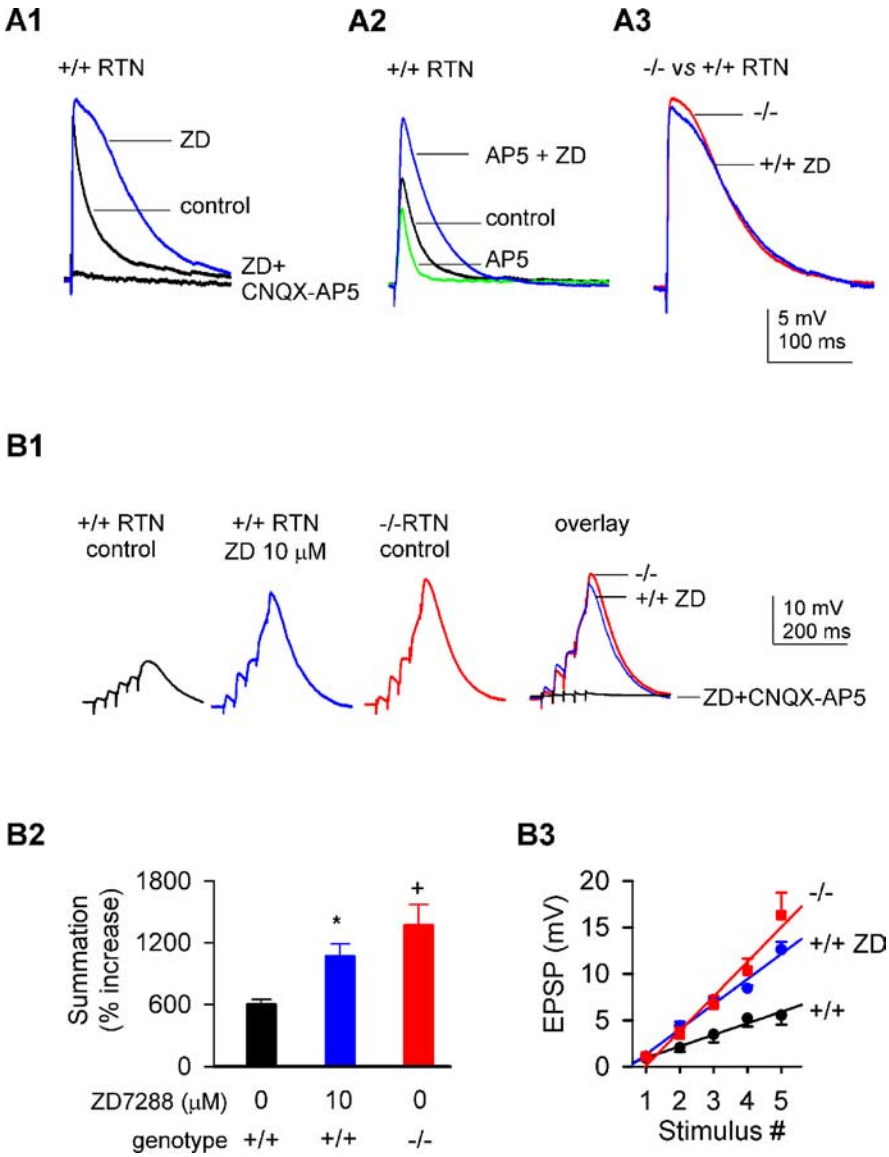

Figure 7. HCN2 constrains ionotropic glutamate receptor-mediated excitatory synaptic responses in RTN neurons. ***A1***, Ionotropic glutamatergic EPSPs were evoked (for details, see Materials and Methods) in the presence of bicuculline and 2-OH-saclofen in a +/+ RTN neuron at −75 mV. ZD7288 (ZD; 10 μM) was added by bath perfusion. The evoked EPSPs could be blocked by CNQX (20 μM) and AP-5 (40 μM). ***A2***, EPSPs mediated by AMPA receptors were isolated by the further addition of AP-5 in a +/+ RTN neuron; ZD7288 (10 μM) was applied by bath perfusion. ***A3***, Comparison of EPSPs in ZD7288 from the same neuron in ***A1*** and from a −/− RTN neuron. ***B1***, A train of EPSPs are evoked in a +/+ RTN neuron by extracellular stimulation of the internal capsule (a train of 5 pulses, 33 Hz, 0.15 ms, every 15 s) in control (no drug) and the presence of ZD7288. In a −/− RTN neuron, EPSPs are evoked in the absence of ZD7288, using the same stimulus protocol. The overlay shows the similarity of −/− EPSPs with +/+ EPSPs in the presence of ZD. Each trace is an average of at least five sweeps. ***B2***, Bar graph for grouped data show percentage increase in EPSP summation in both +/+ and −/− RTN neurons. *$p < 0.05$, ZD7288 (10 μM) versus control (0 μM) in +/+ neurons; $^+p < 0.05$, control +/+ versus control −/−; $n = 10$ each. ***B3***, Plot shows the progressive increase of EPSP amplitude in response to a train of five pulses. Note that the slope of the regression line is shallower in the +/+ control group than in the other two groups.

Single EPSPs were evoked in both +/+ and −/− RTN neurons by electrical stimulation of corticothalamic fibers (single stimuli, every 30 s) in the presence of the $GABA_A$ receptor antagonist bicuculline and the $GABA_B$ receptor antagonist 2-OH-saclofen. Exemplar traces for a +/+ RTN neuron are shown in Figure 7*A*; the evoked EPSPs could be completely abolished by the combination of CNQX and AP-5 but not by AP-5 alone, indicating that the responses were mediated by postsynaptic AMPA and NMDA receptors. In +/+ RTN neurons, addition of ZD7288 significantly increased the duration, peak amplitude, and decay time of EPSPs mediated by both AMPA and NMDA receptors (Table 1). To test the effect of HCN blockade on AMPA receptor-mediated synaptic responses, AP-5 was applied in another group of +/+ RTN neurons (Fig. 7*A2*); application of AP-5 alone decreased EPSP amplitude, half-width duration, and decay time by 35.6 ± 4.5, 28.5 ± 3.2, and 32.2 ± 2.2%, respectively. Addition of ZD7288 significantly increased AMPA receptor-mediated synaptic responses (Table 1).

To examine whether HCN2 deletion had a similar effect on ionotropic glutamate receptor-mediated synaptic responses, EPSPs were recorded from −/− RTN neurons. Because −/− RTN neurons generally fired a burst at membrane potential levels sim-

Table 1. Effects of ZD7288 or HCN2 deletion on single EPSPs in RTN neurons

Genotype	Bath solution	Amplitude (mV)	Rise time (ms)	Half-width (ms)	Decay time (ms)
+/+	Control	7.9 ± 0.6	2.2 ± 0.6	28.9 ± 3.9	75.6 ± 7.5
+/+	ZD7288	10.8 ± 00.7*	1.9 ± 0.4	54.2 ± 7.2*	106.3 ± 10.1*
−/−	Control	10.2 ± 2**	2.3 ± 0.5	52.9 ± 9.3**	115.3 ± 9.5**
+/+	AP-5	5.8 ± 0.5	1.4 ± 0.2	16.6 ± 3.0	49.6 ± 8.1
+/+	AP-5 + ZD7288	9.4 ± 1.5***	1.6 ± 0.2	35.3 ± 5.1***	119.8 ± 9.8***

The first dataset shows effects of ZD7288 or HCN2 deletion on EPSPs mediated by ionotropic glutamate receptors in RTN neurons. Single EPSPs were evoked in RTN neurons by stimulation of corticothalamic fibers (see Materials and Methods) in the presence of bicuculline (10 μM) and 2-OH-saclofen (100 μM) in wild type (+/+) or HCN2 knock-out (−/−) mice. Bath solution, Extracellular bath contains neither ZD7288 nor AP-5 (control), ZD7288 at 10 μM, and/or AP-5 at 40 μM. *$p < 0.05$ versus +/+ control; **$p < 0.05$ versus +/+ control, but $p > 0.05$ versus +/+ ZD7288, one-way ANOVA with Tukey's test; $n = 8$ each. The second dataset shows effects of ZD7288 on EPSPs mediated by AMPA receptors alone. ***$p < 0.05$ versus AP-5 alone, paired t test; $n = 9$.

ilar to those of +/+ RTN neurons, −/− RTN neurons were held at more hyperpolarized membrane potentials (3–6 mV) to evoke single EPSPs so as to permit comparison with those recorded in +/+ RTN neurons. We found that HCN2 deletion also significantly increased amplitude, duration, and decay time of evoked EPSPs (Table 1), and these effects were very similar to those of ZD7288 (Fig. 7*A3*).

The impact of HCN2 expression on synaptic integration in response to corticothalamic stimulation (a train of five pulses, 33 Hz) was also examined; EPSP summation was recorded as described previously (Ying and Goldstein, 2005b). In +/+ RTN neurons, ZD7288 (10 min) markedly increased temporal summation (Fig. 7*B1*). Pooled data (Fig. 7*B2*) demonstrate that the ZD7288-induced increase in summation was significant in +/+ RTN neurons (600 ± 50% in control vs 1070 ± 120% in ZD7288). In the absence of ZD7288, a −/− RTN neuron showed pronounced temporal summation, which was similar to that produced by ZD7288 in +/+ RTN neurons; an example is shown in Figure 7*B1*. All EPSPs could be blocked by bath application of CNQX and AP-5. Group data illustrate that application of ZD7288 or deletion of HCN2 significantly increased EPSP summation in RTN neurons (Fig. 7*B2*).

To compare temporal summation recorded under the three different conditions, the amplitude of individual EPSPs evoked by a five-pulse train were plotted against stimulation number (Fig. 7*B3*). We found that the relationship between EPSP amplitude and stimulus number for control and ZD7288 in +/+ RTN neurons was well described by a straight line, yielding R^2 correlation coefficients of 0.9716 and 0.9808, respectively. In −/− neurons, R^2 was 0.9689. Consistent with the observations above, R_{in} in RTN neurons increased in response to ZD7288 (10 μM) application or HCN2 deletion. For +/+ RTN neurons in the presence of ZD7288, R_{in} was 562 ± 32 MΩ ($n = 16$); for −/− RTN neurons in the absence of ZD7288, R_{in} was 589 ± 35 MΩ ($n = 15$), and the difference between groups is not significant (note that these values were obtained in the absence of NMDA and AMPA receptor antagonists).

I_h constrains excitability mediated by ionotropic glutamate receptor activation in RTN neurons

As shown in Figure 7, I_h block or HCN2 deletion markedly enhanced ionotropic glutamate receptor-mediated synaptic responses in RTN neurons; this suggested that such enhanced synaptic integration might also be accompanied by an increase in spike firing in RTN neurons, thereby increasing GABAergic output to VB neurons. To investigate these possibilities, we compared the effects of ZD7288 on spike firing in RTN neurons and sIPSC frequency in VB neurons in the absence and presence of ionotropic glutamate receptor blockade (Fig. 8). In the example shown (Fig. 8*A1*), superfusion of ZD7288 (10 min) depolarized the membrane potential to approximately −45 mV and dramatically increased the spike firing rate (Fig. 8*A1*, top right). Pooled data (Fig. 8*A2*) shows that ZD7288 significantly increased the firing rate in the absence of glutamatergic blockade. In another group of RTN neurons (Fig. 8*A1*, bottom), addition of ZD7288 did not significantly depolarize the cells (on average, by 2.1 ± 1.2 mV) after a 10 min preapplication of AP-5 plus CNQX, and the effects of ZD7288 on spike firing were significantly attenuated. There was a significant difference in ZD7288-induced effects in the absence and presence of AP-5 plus CNQX (Fig. 8*A2*).

To directly test the effect of I_h block on the spike firing rate in RTN neurons, ZD7288 (20 μM) was included in the recording pipette solution, and the firing rate was measured in the absence or presence of AP-5 plus CNQX. Spike firing during the initial 2 min after rupture of the gigaohm seal was taken as control (Fig. 8*B1*, top left); the firing rate gradually increased and reached a plateau level 12–18 min after obtaining whole-cell configuration (Fig. 8*B1*, top right). In the same cell, subsequent bath application of AP-5 (40 μM) with CNQX (20 μM) markedly attenuated the effect of intracellular ZD7288 on the firing rate (Fig. 8*B1*, bottom left), and firing activity recovered after washout (10 min) of AP-5 plus CNQX (Fig. 8*B1*, bottom right); group data are summarized in Figure 8*B2*. Intracellular application of ZD7288 was associated with a significant increase in R_{in}.

To examine whether the observed increase in firing was coupled to increased GABAergic output to VB neurons, large sIPSC frequency in VB neurons was evaluated in the absence and presence of blockade of ionotropic glutamate receptors. ZD7288 alone increased the large IPSC frequency (Fig. 8*C1*, top); in a different VB neuron, preapplication of AP-5 plus CNQX markedly reduced the ZD7288-induced increase in IPSC frequency (Fig. 8*C1*, bottom). Pooled data are summarized in Figure 8*C2*. Note that there was a significant difference in the response induced by ZD7288 alone and ZD7288 plus ionotropic glutamate antagonists (Fig. 8*A2*,*B2*,*C2*). These data indicate that I_h block enhanced RTN excitability in response to ionotropic glutamate receptor activation, and this increase in excitability augmented GABAergic output from RTN to VB neurons.

HCN2 deletion shifts the input–output curve to the left in RTN neurons

In CA1 pyramidal neurons, in which HCN1 expression is predominant, artificially increasing I_h conductance can markedly decrease tonic spike firing initiated by intracellular depolarizing current pulse injections and shifts the input–output curve to the right (van Welie et al., 2004). Conversely, HCN2 deletion increases tonic spike firing initiated by intracellular depolarizing current pulse injections and shifts the input–output curve to the left in dorsolateral geniculate neurons (Ludwig et al., 2003). To further test the influence of HCN channels alone on intrinsic excitability in RTN neurons, we included ZD7288 (20 μM) in the recording pipette solution and bath applied CNQX (20 μM), AP-5 (40 μM), and gabazine (10 μM) to block fast glutamatergic and GABAergic synaptic transmission. In +/+ RTN neurons, ZD7288 significantly increased input resistance (Table 2) and tonic spike firing initiated by intracellular current steps (Fig. 9*A*); the relationship between injected current and spike frequency

(input–output curve) was shifted to the left by ZD7288 (Fig. 9*B*). The same experiments were performed in HCN2 −/− RTN neurons, and HCN2 deletion abolished ZD7288 effects on intrinsic excitability (Fig. 9*C*,*D*, Table 2). These results indicate the HCN2 contributes to the intrinsic excitability and spike firing of RTN neurons in the absence of synaptic input.

HCN2 channels and GluR4-containing AMPA receptors are present in dendritic spines

The data strongly suggest that I_h conducted by HCN2 channels acts as a "leak current path" to shunt excitatory inputs (Robinson and Siegelbaum, 2003). Such a phenomenon implies that HCN2 channels and glutamate receptors might be in close proximity to one another, because both HCN2 channels (Abbas et al., 2006) and glutamate receptors containing the GluR4 subunit (Golshani et al., 2001) appear to be present in the dendritic spines of RTN neurons. To further investigate this relationship, we examined whether HCN2 and the AMPA receptor GluR4 subunit colocalized in dendritic spines using triple-labeling immunofluorescence and confocal microscopy (Fig. 10). We focused on AMPA receptor GluR4 subunit expression because the GluR4 subunit is preferentially expressed at corticothalamic synapses in the RTN (Mineff and Weinberg, 2000; Golshani et al., 2001). GluR4-IR was clearly evident in RTN (Fig. 10*A1*,*A2*). Immunoreactivities for HCN2 and the dendritic spine marker cortactin colocalized (Fig. 10*B1*,*C1*), and the pattern of HCN2 distribution seen here is consistent with our previous observations (Abbas et al., 2006). GluR4- and cortactin-IR overlapped (Fig. 10*B2*,*C2*), consistent with the expression of GluR4 in dendritic spines; in the same slice, fluorescent signals for HCN2 and GluR4 also overlapped (Fig. 10*B3*,*C3*). The merged image clearly demonstrates that signals for GluR4, cortactin, and HCN2 colocalize (Fig. 10*B4*,*C4*), indicating that HCN2 and GluR4 are located in the dendritic spines of RTN neurons.

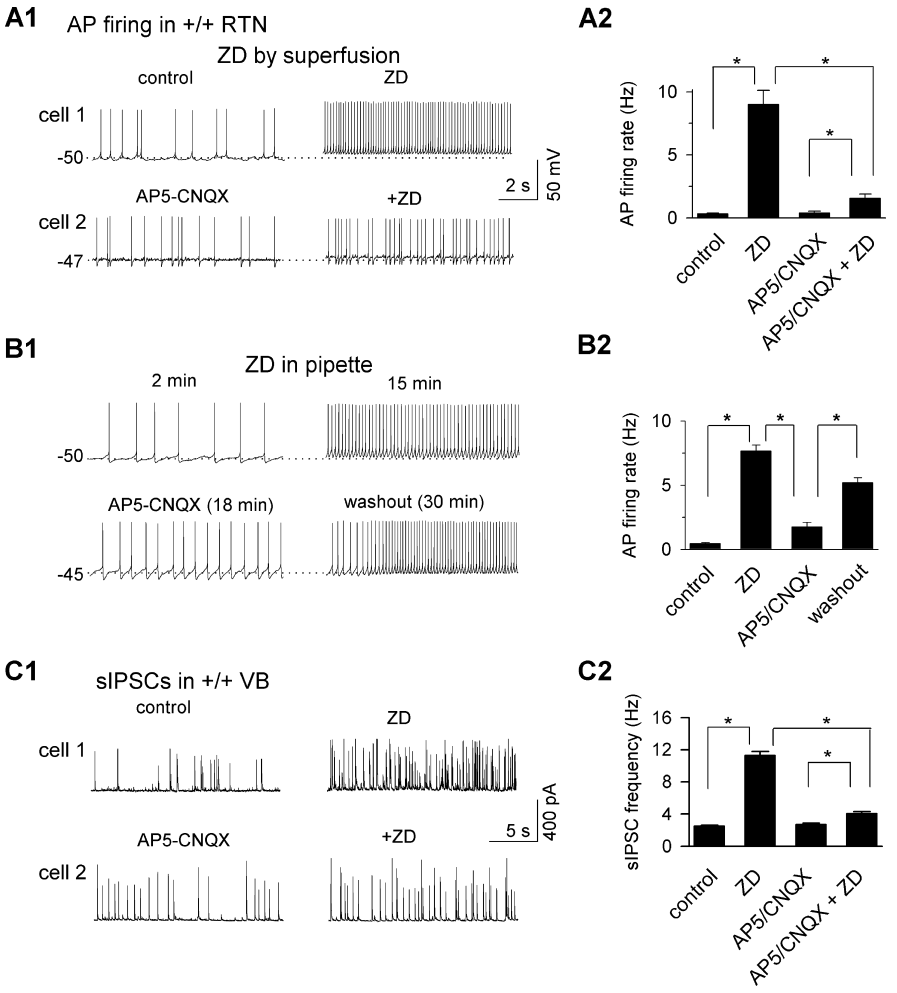

Figure 8. Blockade of ionotropic glutamate receptors attenuates response to ZD7288. ***A1***, Preblockade of ionotropic glutamatergic receptors markedly attenuates excitatory effects of ZD7288 (ZD) on spike firing in RTN neurons. Representative segments of the voltage trace show spike firing in control (no drug; top left) and bath application of ZD7288 (20 μM) alone (top right) in an RTN neuron. The membrane potential (in millivolts; indicated at left) is the average membrane potential between spikes (here and in ***B1***). Note the depolarization in the membrane potential after superfusion of ZD7288. Traces below (in a different neuron than above) show firing in the presence of bath-applied AP-5 (40 μM) plus CNQX (20 μM) and followed by AP-5 plus CNQX plus ZD7288 (20 μM). ***A2***, Bar graph summarizing the effects of bath-applied ZD7288 on spike firing rate in the absence or presence of AP-5 plus CNQX in RTN neurons. $^*p < 0.05$, one-way ANOVA; $n = 8$ per group (in which "group" is without or with AP-5 plus CNQX). ***B1***, Representative traces demonstrating spike firing in a different RTN neuron than in ***A***. Here ZD7288 (20 μM) was present in the recording pipette solution; the first trace (top left) shows spike firing within the first 2 min after obtaining whole-cell configuration, and firing is markedly increased 15 min later (top right). Again, there is a small depolarization in the membrane potential in the presence of ZD7288. Bath application of AP-5 plus CNQX for 5 min markedly decreased spike firing (bottom left); after AP-5 plus CNQX washout (10 min), firing activity recovered (bottom right). Times indicated are relative to seal rupture. ***B2***, Bar graph summarizing the effects of intracellularly applied ZD7288 on spike firing rate before and after AP-5 plus CNQX superfusion in RTN neurons. The effect of ZD7288 on spike firing was markedly reduced by AP-5 plus CNQX application. $^*p < 0.05$, one-way ANOVA; $n = 14$ cells. ***C1***, Preapplication of AP-5 plus CNQX markedly attenuated the effects of ZD7288 on the frequency of large (>100 pA) sIPSCs in VB neurons. ***C2***, Bar graph summarizing the effects of bath-applied ZD7288 on large sIPSC frequency in the absence or presence of AP-5 plus CNQX in VB neurons. $^*p < 0.05$, one-way ANOVA; $n = 10$ per group (as defined in ***A2***).

Discussion

Multiple ionic conductances have been identified in RTN neurons (Avanzini et al., 1989; Bal and McCormick, 1993; Pinault, 2004), including I_h as reported recently by us (Abbas et al., 2006) and others (Rateau and Ropert, 2006). The influence of I_h on overall cellular excitability is dependent on at least two major factors, channel isoform and subcellular distribution (Chaplan et al., 2003; Strauss et al., 2004; Fan et al., 2005). This study focused on identifying the major HCN channel isoform underlying the generation of I_h and regulation of excitability in mouse RTN neurons. The key findings are that HCN2 is the major isoform, and functional expression of HCN2 constrains intrinsic excitability and excitatory synaptic integration, in RTN neurons.

HCN2 is the major functional isoform in RTN neurons

HCN2 and HCN4 channels are likely to be the most abundant isoforms in the RTN (Monteggia et al., 2000; Santoro et al., 2000; Notomi and Shigemoto, 2004). We combined electrophysiological, pharmacological, gene knock-out, and immunohistological techniques to identify the functional HCN isoform in RTN neurons. In RTN neurons from HCN2 null mice (HCN2 −/−), no apparent I_h was detected, even using a 20 s voltage step to −110

Table 2. Effects of ZD7288 or HCN2 deletion on input resistance in RTN neurons

Genotype	Bath solution	Input resistance (MΩ)
+/+	Control	337 ± 22
+/+	ZD7288	564 ± 27*
−/−	Control	643 ± 76*
−/−	ZD7288	669 ± 110*

*$p < 0.05$ versus +/+ control (0 μM ZD7288), ANOVA with Tukey's test for pairwise comparison; $n = 16$ each. ZD7288 (20 μM) was applied by bath perfusion or was included in recording pipette. These data were obtained in the presence of CNQX, AP-5, and gabazine.

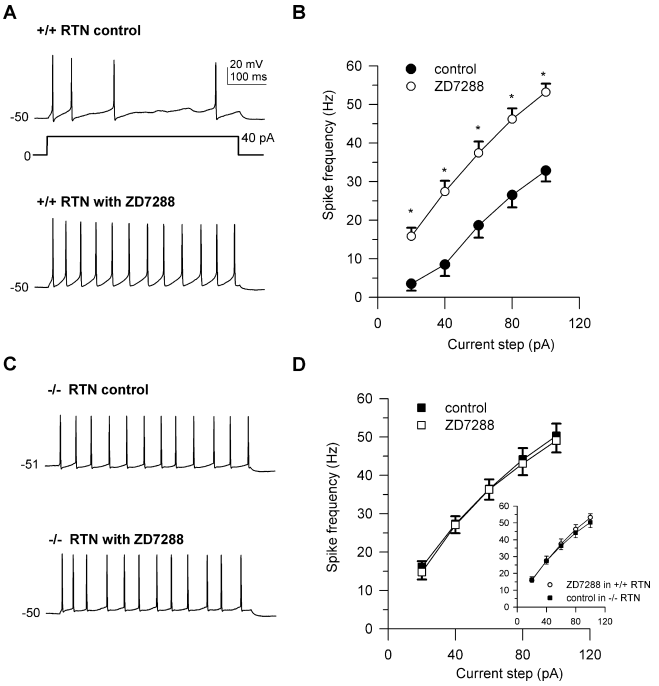

Figure 9. HCN2 deletion abolishes effects of ZD7288 on tonic spike firing in RTN neurons. ***A***, Representative traces demonstrating tonic spike firing initiated by intracellular injection of current pulses in two different +/+ RTN neurons in the absence (control) or presence of ZD7288 (20 μM in patch-clamp recording pipette). All the traces in ***A*** and ***C*** were initiated with the same current protocol (shown below); initial holding potential (in millivolts) is indicated to the left of each trace. AP-5 (40 μM), CNQX (20 μM), and gabazine (10 μM) were present in the extracellular bath solution here and in ***C***. ***B***, Grouped data indicate that ZD7288 shifts the input–output curve to left in +/+ RTN neurons. *$p < 0.05$ versus control ($n = 12$ per each group; unpaired *t* test). ***C***, The same experiment as depicted in ***A*** was performed in HCN2 −/− RTN neurons. ZD7288 did not increase spike firing. ***D***, Grouped data demonstrate lack of effect of ZD7288 on HCN2 −/− RTN neurons ($n = 13$ per each group). Inset, Comparison of input–output curves between +/+ RTN neurons in the presence of ZD7288 and −/− RTN neurons under control conditions (no ZD7288).

mV (Fig. 3*E2*), although HCN4 expression remained unchanged (Fig. 3*C2*). TRIP8b (for TPR-containing Rab8b interacting protein) (Santoro et al., 2004) and N-linked glycosylation (Much et al., 2003) have been shown to help direct HCN channels to the cell surface; although HCN4 appears to be present in RTN neurons, it may not be functionally incorporated into the plasma membrane as a result of a failure of trafficking, and this possibility remains to be explored.

HCN2 and HCN4 channels are highly sensitive to modulation by intracellular cAMP (Ludwig et al., 1998; Chen et al., 2001b; Ulens and Tytgat, 2001; Wainger et al., 2001); however, 8-Br-cAMP, which can increase I_h (Gasparini and DiFrancesco, 1999; Cuttle et al., 2001), decreased GABAergic output from HCN2 +/+, but not −/−, RTN neurons (Fig. 5). Lamotrigine, which also increases the I_h conductance (Poolos et al., 2002), mimicked the effects of 8-Br-cAMP (Fig. 5). Because the RTN is the sole source of GABAergic input to the VB in rodents (Arcelli et al., 1997), an increase in large sIPSC frequency indicates that there is an increase in spike firing in the RTN. Consistent with those observations, intracellular perfusion of ZD7288 increased intrinsic excitability in HCN2 +/+, but not −/−, neurons (Fig. 9). These data strongly suggest that HCN2, but not HCN4, is involved in determining I_h-related excitability in RTN neurons.

Because HCN1 and HCN3 are weakly expressed in the RTN (Moosmang et al., 1999; Notomi and Shigemoto, 2004), HCN1 (and possibly HCN3) channels might generate a distal dendritic I_h that was undetectable at the soma of HCN2 −/− RTN neurons as a consequence of dendritic filtering resulting from a large electrotonic length constant (Destexhe et al., 1996). However, HCN2 deletion abolished effects of ZD7288 on R_{in} (Table 2), spike firing (Fig. 9*D*), and evoked synaptic responses (Fig. 7, Table 1). It is unlikely, therefore, that dendritic filtering obscured the detection of I_h-dependent properties mediated by other functional HCN channels.

The increased excitability of RTN neurons attributable to either I_h block (Figs. 1, 6, 8) or HCN2 deletion (Figs. 4, 9) resulted in a marked increase in large-amplitude sIPSC frequency in VB neurons (Figs. 2, 4, 8), consistent with a presynaptic action. In regions with significant HCN1 expression, such as the stratum oriens in the hippocampus (Notomi and Shigemoto, 2004), however, ZD7288 decreases sIPSC frequency (Lupica et al., 2001). This, then, raises the question: why does I_h have divergent effects on excitability in different brain regions? We address this question in the following sections.

HCN2 regulates excitatory synaptic integration in RTN neurons

Expression of HCN2 channels in RTN dendrites markedly constrained integration of corticothalamic-evoked EPSP mediated by ionotropic glutamate receptors (Fig. 7, Table 1). The AMPA receptor GluR4 subunit is preferentially expressed at corticothalamic synapses in the RTN (Mineff and Weinberg, 2000; Golshani et al., 2001), and we demonstrated previously that the HCN2 channel is densely expressed in dendritic spines (Abbas et al., 2006). Here, we found that immunoreactivities for GluR4 and HCN2 were colocalized in dendritic spines (Fig. 10), thereby providing a molecular basis for a possible interaction between conductances mediated by HCN2 channels and GluR4-containing AMPA receptors.

Increased I_h (Fan et al., 2005) or HCN1 channel expression (Nolan et al., 2004) decreases intrinsic and synaptic excitability through a current leak path (Robinson and Siegelbaum, 2003), which presumably occurs at the dendritic level; conversely, I_h block enhances both excitability and EPSP responses, which can be attributed to an increase in R_{in} (Magee, 1998; Williams and Stuart, 2000; Berger et al., 2001; Kole et al., 2006). Functional expression of dendritic RTN HCN2 channels appears to recapitulate many aspects of dendritic HCN1 function seen in other brain areas. For example, increases in R_{in}, attributable to either I_h block or HCN2 deletion (Table 2), increased EPSP time course and amplitude (Fig. 7, Table 1), consistent with the existence of an HCN2-dependent leak pathway under physiological conditions. These data lead us to conclude that HCN2 expression constrains glutamate-driven excitability via a dendritic shunting mechanism.

Possible mechanisms underlying excitatory effects attributable to I_h block or HCN2 deletion

ZD7288-induced membrane hyperpolarization, as seen in VB neurons (Fig. 1*B*), is a well described phenomenon resulting from I_h block and is accompanied by a decrease in spike firing (Fig. 1*B*). Conversely, ZD7288 induced a novel moderate, but significant, depolarization in RTN neurons (which was accompanied by an increase in spike firing) (Figs. 1, 8*A1*), and this may be attributable to enhanced spread of dendritic depolarization(s) to the soma. This suggests that I_h may serve distinct functions in RTN and VB neurons. I_h has been shown to regulate tonic action potential firing in entorhinal cortex pyramidal cells (Rosenkranz and Johnston, 2006) and striatal cholinergic interneurons (Deng et al., 2007). Here, ZD7288 effects on tonic single spike firing were observed at relatively depolarized membrane potentials (approximately −50 mV) (Fig. 9). This is not altogether surprising when one considers that HCN2 channels are partially open at this potential (Chen et al., 2001a) and may generate a voltage-independent current (Proenza et al., 2002; Macri and Accili, 2004; Proenza and Yellen, 2006). Another possible explanation for this effect is poor dendritic voltage control when recording from the soma, which could result from the nonisopotentiality of RTN neurons (Destexhe et al., 1996). ZD7288-mediated excitation in RTN was unlikely to result from the ZD7288 block of the potassium conductances tested here (Fig. 6) because ZD7288-induced increases in firing persisted in the presence of Ba^{2+} or bupivacaine, which block TWIK (tandem of P-domains in weak inward rectifying K^+ channel) and TASK potassium channels (Patel and Honoré, 2001; Lesage, 2003; Meuth et al., 2003), or dequalinium, which blocks SK channels (Strøbaek et al., 2000).

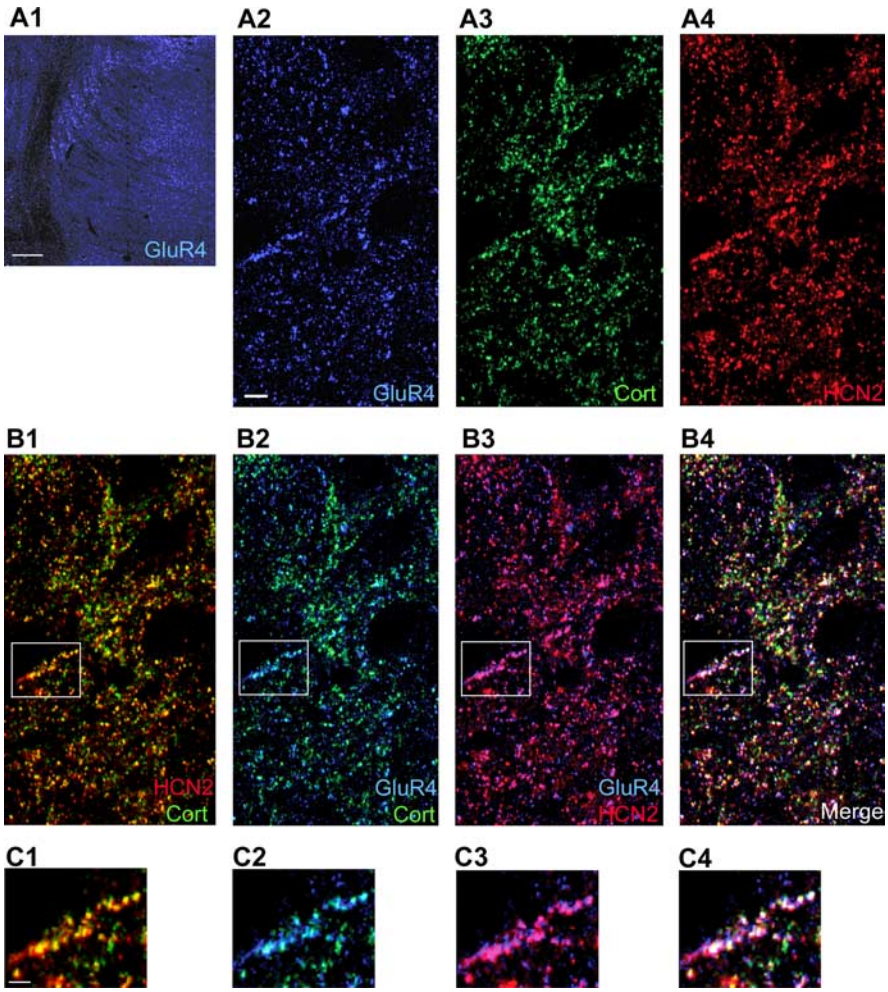

Figure 10. HCN2 colocalizes with GluR4 in dendritic spines of RTN neurons. ***A1***, A high level of AMPA receptor subunit 4 (GluR4, blue) immunoreactivity is detected in the RTN. Scale bars: ***A1***, 200 μm; ***A2–A4***, ***B1–B4***, 5 μm; ***C1–C4***, 2 μm. ***A2–A4***, A high-magnification confocal fluorescence micrograph shows strong punctate immunofluorescence corresponding to GluR4 (***A2***), cortactin (Cort; green, ***A3***), and HCN2 (red, ***A4***) in +/+ RTN neurons. ***B1***, Overlay of images in ***A3*** and ***A4***. Yellow represents regions of apparent colocalization of cortactin with HCN2 immunofluorescent signals. ***B2***, Overlay image shows that GluR4-immunoreactive puncta in ***A2*** colocalize with that for cortactin-IR in ***A3***, suggesting that GluR4 subunits are expressed in dendritic spines of +/+ RTN neurons. The cyan signal indicates overlap of the GluR4 signal with that of cortactin. ***B3***, GluR4-immunoreactive puncta in ***A2*** also colocalize with HCN2-IR in ***A4***. The overlap between HCN2 and GluR4 signal is shown in magenta. ***B4***, GluR4- and HCN2-IRs overlap with that of cortactin (white), indicating that GluR4 colocalizes with HCN2 in dendritic spines. ***C1–C4***, High-magnification view of ***B1–B4*** boxed regions showing colocalization of HCN2- with cortactin-IR (***C1***) and GluR4-IR colocalization with either cortactin-IR (***C2***) or HCN2-IR (***C3***). A number of structures resembling dendritic spines (***C4***, white) show colocalization of GluR4-, HCN2-, and cortactin-IR.

In CA1 pyramidal cells, I_h block removes dendritic shunting, improves dendrosomatic coupling, and facilitates spread of membrane depolarization from distal dendrites to the soma (Golding et al., 2005). In RTN neurons, such depolarization can result from fast excitatory transmission originating in the massive corticothalamic input to the RTN (Steriade et al., 1997). Concordant with these facts is the observation that the ZD7288-induced increase in RTN spike firing was dramatically reduced, and the associated depolarization was insignificant, in the presence of AP-5 plus CNQX (Fig. 8*A*). Thus, regulation of dendritic I_h likely permits scaling of glutamate-mediated depolarization in RTN neurons.

ZD7288 application or HCN2 deletion induced the "burst" large-amplitude sIPSC pattern in VB neurons (Figs. 2, 4, 5), and this pattern could result from burst spike firing in RTN neurons that occurs as a consequence of a high-density dendritic T-type Ca^{2+} current (I_T) (Destexhe et al., 1996). The depolarization during I_h block may facilitate RTN low-threshold Ca^{2+} spikes firing because the I_T underlying RTN bursting activates at depolarized potentials (Huguenard and Prince, 1992). Conceivably, ZD7288-induced depolarization brings the membrane potential of RTN neurons closer to burst firing threshold (Destexhe et al., 1996), whereas enhanced excitatory synaptic integration (in HCN2 null mice) may directly induce the Ca^{2+} spike (Destexhe et al., 1994; Warren et al., 1994), but additional work is needed to clarify the underlying mechanism(s). Consistent with this overall interpretation is the observation that HCN2 deletion produces both oscillatory Ca^{2+} transients and burst spike firing in thalamic dorsolateral geniculate neurons (Ludwig et al., 2003) and burst spike firing in RTN neurons (Ying et al., 2006b). Similarly, other studies report that HCN1 deletion or ZD7288 application prolongs both dendritic Ca^{2+} signals and membrane depolariza-

tion (Tsay and Siegelbaum, 2006) and increases Ca^{2+} spike firing (Berger et al., 2003; Kole et al., 2007).

In summary, we examined the role of HCN2 expression in regulating intrinsic excitability and integration of excitatory synaptic input in thalamic circuits. Our results indicate that HCN2 is the primary functional HCN isoform, which effectively controls GABAergic output via distal dendritic I_h in RTN neurons. Thus, the physiologic function of I_h is highly related to the pattern of compartmental distribution in a specific population of neurons. The present results should be useful for understanding how I_h mediates excitatory responses in one region and inhibitory responses in another.

References

Abbas SY, Ying SW, Goldstein PA (2006) Compartmental distribution of hyperpolarization-activated cyclic-nucleotide-gated channel 2 and hyperpolarization-activated cyclic-nucleotide-gated channel 4 in thalamic reticular and thalamocortical relay neurons. Neuroscience 141:1811–1825.

Arcelli P, Frassoni C, Regondi MC, De Biasi S, Spreafico R (1997) GABAergic neurons in mammalian thalamus: a marker of thalamic complexity? Brain Res Bull 42:27–37.

Avanzini G, de Curtis M, Panzica F, Spreafico R (1989) Intrinsic properties of nucleus reticularis thalami neurones of the rat studied *in vitro*. J Physiol (Lond) 416:111–122.

Bal T, McCormick DA (1993) Mechanisms of oscillatory activity in guinea-pig nucleus reticularis thalami *in vitro*: a mammalian pacemaker. J Physiol (Lond) 468:669–691.

Berger T, Lüscher HR (2004) Associative somatodendritic interaction in layer V pyramidal neurons is not affected by the antiepileptic drug lamotrigine. Eur J Neurosci 20:1688–1693.

Berger T, Larkum ME, Lüscher HR (2001) High I_h channel density in the distal apical dendrite of layer V pyramidal cells increases bidirectional attenuation of EPSPs. J Neurophysiol 85:855–868.

Berger T, Senn W, Lüscher HR (2003) Hyperpolarization-activated current I_h disconnects somatic and dendritic spike initiation zones in layer V pyramidal neurons. J Neurophysiol 90:2428–2437.

Carlisle HJ, Kennedy MB (2005) Spine architecture and synaptic plasticity. Trends Neurosci 28:182–187.

Chaplan SR, Guo HQ, Lee DH, Luo L, Liu C, Kuei C, Velumian AA, Butler MP, Brown SM, Dubin AE (2003) Neuronal hyperpolarization-activated pacemaker channels drive neuropathic pain. J Neurosci 23:1169–1178.

Chen J, Mitcheson JS, Tristani-Firouzi M, Lin M, Sanguinetti MC (2001a) The S4–S5 linker couples voltage sensing and activation of pacemaker channels. Proc Natl Acad Sci USA 98:11277–11282.

Chen S, Wang J, Siegelbaum SA (2001b) Properties of hyperpolarization-activated pacemaker current defined by coassembly of HCN1 and HCN2 subunits and basal modulation by cyclic nucleotide. J Gen Physiol 117:491–504.

Cuttle MF, Rusznak Z, Wong AY, Owens S, Forsythe ID (2001) Modulation of a presynaptic hyperpolarization-activated cationic current (I_h) at an excitatory synaptic terminal in the rat auditory brainstem. J Physiol (Lond) 534:733–744.

Deng P, Zhang Y, Xu ZC (2007) Involvement of I_h in dopamine modulation of tonic firing in striatal cholinergic interneurons. J Neurosci 27:3148–3156.

Destexhe A, Contreras D, Sejnowski TJ, Steriade M (1994) A model of spindle rhythmicity in the isolated thalamic reticular nucleus. J Neurophysiol 72:803–818.

Destexhe A, Contreras D, Steriade M, Sejnowski TJ, Huguenard JR (1996) *In vivo*, *in vitro*, and computational analysis of dendritic calcium currents in thalamic reticular neurons. J Neurosci 16:169–185.

Fan Y, Fricker D, Brager DH, Chen X, Lu HC, Chitwood RA, Johnston D (2005) Activity-dependent decrease of excitability in rat hippocampal neurons through increases in I_h. Nat Neurosci 8:1542–1551.

Gasparini S, DiFrancesco D (1999) Action of serotonin on the hyperpolarization-activated cation current (I_h) in rat CA1 hippocampal neurons. Eur J Neurosci 11:3093–3100.

Gauss R, Seifert R (2000) Pacemaker oscillations in heart and brain: a key role for hyperpolarization-activated cation channels. Chronobiol Int 17:453–469.

Golding NL, Mickus TJ, Katz Y, Kath WL, Spruston N (2005) Factors mediating powerful voltage attenuation along CA1 pyramidal neuron dendrites. J Physiol (Lond) 568:69–82.

Golshani P, Liu XB, Jones EG (2001) Differences in quantal amplitude reflect GluR4-subunit number at corticothalamic synapses on two populations of thalamic neurons. Proc Natl Acad Sci USA 98:4172–4177.

Hering H, Sheng M (2001) Dendritic spines: structure, dynamics and regulation. Nat Rev Neurosci 2:880–888.

Huguenard JR, Prince DA (1992) A novel T-type current underlies prolonged Ca^{2+}-dependent burst firing in GABAergic neurons of rat thalamic reticular nucleus. J Neurosci 12:3804–3817.

Ishii TM, Takano M, Ohmori H (2001) Determinants of activation kinetics in mammalian hyperpolarization-activated cation channels. J Physiol (Lond) 537:93–100.

Kasai H, Matsuzaki M, Noguchi J, Yasumatsu N, Nakahara H (2003) Structure-stability-function relationships of dendritic spines. Trends Neurosci 26:360–368.

Koch U, Grothe B (2003) Hyperpolarization-activated current (I_h) in the inferior colliculus: distribution and contribution to temporal processing. J Neurophysiol 90:3679–3687.

Kole MH, Hallermann S, Stuart GJ (2006) Single I_h channels in pyramidal neuron dendrites: properties, distribution, and impact on action potential output. J Neurosci 26:1677–1687.

Kole MH, Bräuer AU, Stuart GJ (2007) Inherited cortical HCN1 channel loss amplifies dendritic calcium electrogenesis and burst firing in a rat absence epilepsy model. J Physiol (Lond) 578:507–525.

Lesage F (2003) Pharmacology of neuronal background potassium channels. Neuropharmacology 44:1–7.

Lörincz A, Notomi T, Tamás G, Shigemoto R, Nusser Z (2002) Polarized and compartment-dependent distribution of HCN1 in pyramidal cell dendrites. Nat Neurosci 5:1185–1193.

Ludwig A, Zong X, Jeglitsch M, Hofmann F, Biel M (1998) A family of hyperpolarization-activated mammalian cation channels. Nature 393:587–591.

Ludwig A, Zong X, Stieber J, Hullin R, Hofmann F, Biel M (1999) Two pacemaker channels from human heart with profoundly different activation kinetics. EMBO J 18:2323–2329.

Ludwig A, Budde T, Stieber J, Moosmang S, Wahl C, Holthoff K, Langebartels A, Wotjak C, Munsch T, Zong X, Feil S, Feil R, Lancel M, Chien KR, Konnerth A, Pape HC, Biel M, Hofmann F (2003) Absence epilepsy and sinus dysrhythmia in mice lacking the pacemaker channel HCN2. EMBO J 22:216–224.

Lupica CR, Bell JA, Hoffman AF, Watson PL (2001) Contribution of the hyperpolarization-activated current (I_h) to membrane potential and GABA release in hippocampal interneurons. J Neurophysiol 86:261–268.

Macri V, Accili EA (2004) Structural elements of instantaneous and slow gating in hyperpolarization-activated cyclic nucleotide-gated channels. J Biol Chem 279:16832–16846.

Magee JC (1998) Dendritic hyperpolarization-activated currents modify the integrative properties of hippocampal CA1 pyramidal neurons. J Neurosci 18:7613–7624.

Magee JC (1999) Dendritic I_h normalizes temporal summation in hippocampal CA1 neurons. Nat Neurosci 2:508–514.

Meuth SG, Budde T, Kanyshkova T, Broicher T, Munsch T, Pape HC (2003) Contribution of TWIK-related acid-sensitive K^+ channel 1 (TASK1) and TASK3 channels to the control of activity modes in thalamocortical neurons. J Neurosci 23:6460–6469.

Mineff EM, Weinberg RJ (2000) Differential synaptic distribution of AMPA receptor subunits in the ventral posterior and reticular thalamic nuclei of the rat. Neuroscience 101:969–982.

Mokin M, Keifer J (2006) Quantitative analysis of immunofluorescent punctate staining of synaptically localized proteins using confocal microscopy and stereology. J Neurosci Methods 157:218–224.

Monteggia LM, Eisch AJ, Tang MD, Kaczmarek LK, Nestler EJ (2000) Cloning and localization of the hyperpolarization-activated cyclic nucleotide-gated channel family in rat brain. Brain Res Mol Brain Res 81:129–139.

Moosmang S, Biel M, Hofmann F, Ludwig A (1999) Differential distribution of four hyperpolarization-activated cation channels in mouse brain. Biol Chem 380:975–980.

Much B, Wahl-Schott C, Zong X, Schneider A, Baumann L, Moosmang S,

Ludwig A, Biel M (2003) Role of subunit heteromerization and *N*-linked glycosylation in the formation of functional hyperpolarization-activated cyclic nucleotide-gated channels. J Biol Chem 278:43781–43786.

Nagy A, Gerstsenstein M, Vintersten K, Behringer B (2003) Manipulating the mouse embryo: a laboratory manual, Ed 3. Cold Spring Harbor, NY: Cold Spring Harbor Laboratory.

Nimchinsky EA, Sabatini BL, Svoboda K (2002) Structure and function of dendritic spines. Annu Rev Physiol 64:313–353.

Nolan MF, Malleret G, Dudman JT, Buhl DL, Santoro B, Gibbs E, Vronskaya S, Buzsaki G, Siegelbaum SA, Kandel ER, Morozov A (2004) A behavioral role for dendritic integration: HCN1 channels constrain spatial memory and plasticity at inputs to distal dendrites of CA1 pyramidal neurons. Cell 119:719–732.

Notomi T, Shigemoto R (2004) Immunohistochemical localization of I_h channel subunits, HCN1–4, in the rat brain. J Comp Neurol 471:241–276.

Pape HC (1996) Queer current and pacemaker: the hyperpolarization-activated cation current in neurons. Annu Rev Physiol 58:299–327.

Patel AJ, Honoré E (2001) Properties and modulation of mammalian 2P domain K^+ channels. Trends Neurosci 24:339–346.

Pinault D (2004) The thalamic reticular nucleus: structure, function and concept. Brain Res Brain Res Rev 46:1–31.

Poolos NP, Migliore M, Johnston D (2002) Pharmacological upregulation of h-channels reduces the excitability of pyramidal neuron dendrites. Nat Neurosci 5:767–774.

Proenza C, Yellen G (2006) Distinct populations of HCN pacemaker channels produce voltage-dependent and voltage-independent currents. J Gen Physiol 127:183–190.

Proenza C, Angoli D, Agranovich E, Macri V, Accili EA (2002) Pacemaker channels produce an instantaneous current. J Biol Chem 277:5101–5109.

Rateau Y, Ropert N (2006) Expression of a functional hyperpolarization-activated current I_h in the mouse nucleus reticularis thalami. J Neurophysiol 95:3073–3085.

Robinson RB, Siegelbaum SA (2003) Hyperpolarization-activated cation currents: from molecules to physiological function. Annu Rev Physiol 65:453–480.

Rosenkranz JA, Johnston D (2006) Dopaminergic regulation of neuronal excitability through modulation of I_h in layer V entorhinal cortex. J Neurosci 26:3229–3244.

Santoro B, Chen S, Lüthi A, Pavlidis P, Shumyatsky GP, Tibbs GR, Siegelbaum SA (2000) Molecular and functional heterogeneity of hyperpolarization-activated pacemaker channels in the mouse CNS. J Neurosci 20:5264–5275.

Santoro B, Wainger BJ, Siegelbaum SA (2004) Regulation of HCN channel surface expression by a novel C-terminal protein-protein interaction. J Neurosci 24:10750–10762.

Segal M (2005) Dendritic spines and long-term plasticity. Nat Rev Neurosci 6:277–284.

Seifert R, Scholten A, Gauss R, Mincheva A, Lichter P, Kaupp UB (1999) Molecular characterization of a slowly gating human hyperpolarization-activated channel predominantly expressed in thalamus, heart, and testis. Proc Natl Acad Sci USA 96:9391–9396.

Steriade M, Jones EG, McCormick DA (1997) Thalamus. Oxford, UK: Elsevier Science.

Stieber J, Thomer A, Much B, Schneider A, Biel M, Hofmann F (2003) Molecular basis for the different activation kinetics of the pacemaker channels HCN2 and HCN4. J Biol Chem 278:33672–33680.

Strauss U, Kole MH, Bräuer AU, Pahnke J, Bajorat R, Rolfs A, Nitsch R, Deisz RA (2004) An impaired neocortical I_h is associated with enhanced excitability and absence epilepsy. Eur J Neurosci 19:3048–3058.

Strøbaek D, Jørgensen TD, Christophersen P, Ahring PK, Olesen SP (2000) Pharmacological characterization of small-conductance Ca^{2+}-activated K^+ channels stably expressed in HEK 293 cells. Br J Pharmacol 129:991–999.

Stuart G, Spruston N (1998) Determinants of voltage attenuation in neocortical pyramidal neuron dendrites. J Neurosci 18:3501–3510.

Tsay D, Siegelbaum SA (2006) HCN1 KO mice exhibit enhanced calcium flux in distal dendrites of CA1 pyramidal neurons. Soc Neurosci Abstr 32:334.10.

Tsay D, Yuste R (2004) On the electrical function of dendritic spines. Trends Neurosci 27:77–83.

Ulens C, Tytgat J (2001) Functional heteromerization of HCN1 and HCN2 pacemaker channels. J Biol Chem 276:6069–6072.

van Welie I, van Hooft JA, Wadman WJ (2004) Homeostatic scaling of neuronal excitability by synaptic modulation of somatic hyperpolarization-activated I_h channels. Proc Natl Acad Sci USA 101:5123–5128.

Wainger BJ, DeGennaro M, Santoro B, Siegelbaum SA, Tibbs GR (2001) Molecular mechanism of cAMP modulation of HCN pacemaker channels. Nature 411:805–810.

Warren RA, Agmon A, Jones EG (1994) Oscillatory synaptic interactions between ventroposterior and reticular neurons in mouse thalamus *in vitro*. J Neurophysiol 72:1993–2003.

Williams SR, Stuart GJ (2000) Site independence of EPSP time course is mediated by dendritic I_h in neocortical pyramidal neurons. J Neurophysiol 83:3177–3182.

Ying SW, Goldstein PA (2005a) Propofol-block of SK channels in reticular thalamic neurons enhances GABAergic inhibition in relay neurons. J Neurophysiol 93:1935–1948.

Ying SW, Goldstein PA (2005b) Propofol suppresses synaptic responsiveness of somatosensory relay neurons to excitatory input by potentiating $GABA_A$ receptor chloride channels. Mol Pain 1:2.

Ying SW, Abbas SY, Harrison NL, Goldstein PA (2006a) Propofol block of I_h contributes to the suppression of neuronal excitability and rhythmic burst firing in thalamocortical neurons. Eur J Neurosci 23:465–480.

Ying SW, Jia F, Abbas SY, Ludwig A, Goldstein PA (2006b) HCN channels are crucial for excitability and firing patterns in reticular thalamic neurons. Soc Neurosci Abstr 32:334.5.

Yuste R, Tank DW (1996) Dendritic integration in mammalian neurons, a century after Cajal. Neuron 16:701–716.